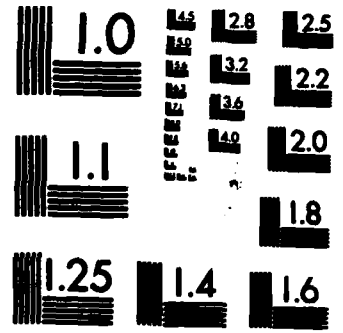
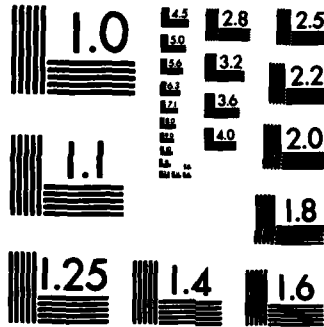


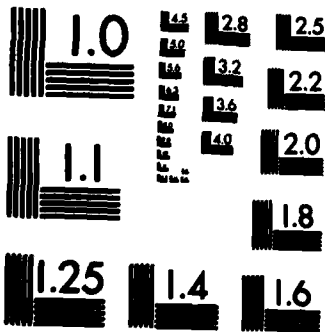
MICROCOPY RESOLUTION TEST CHART
NATIONAL BUREAU OF STANDARDS-1963-A



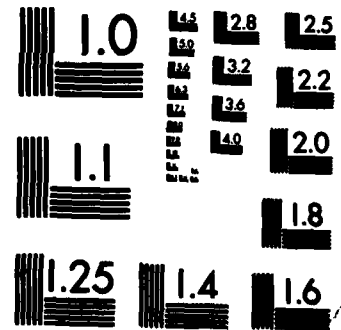
MICROCOPY RESOLUTION TEST CHART
NATIONAL BUREAU OF STANDARDS-1963-A



MICROCOPY RESOLUTION TEST CHART
NATIONAL BUREAU OF STANDARDS-1963-A



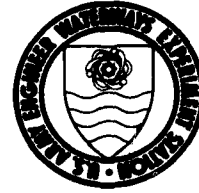
MICROCOPY RESOLUTION TEST CHART
NATIONAL BUREAU OF STANDARDS-1963-A



MICROCOPY RESOLUTION TEST CHART
NATIONAL BUREAU OF STANDARDS-1963-A



2



MISCELLANEOUS PAPER SL-82-10

THE HEMSS 3T EXPERIMENT

by

Anthony A. Bombich

Structures Laboratory

U. S. Army Engineer Waterways Experiment Station
P. O. Box 631, Vicksburg, Miss. 39180

AD A 120669

July 1982
Final Report

OCT 25 1982

Approved For Public Release; Distribution Unlimited

A



DTC FILE C

Prepared for Defense Nuclear Agency
Washington, D. C. 20305

Under DNA Subtask Y99QAXSD070

82 10 25 023

**Destroy this report when no longer needed. Do not return
it to the originator.**

**The findings in this report are not to be construed as an official
Department of the Army position unless so designated,
by other authorized documents.**

**The contents of this report are not to be used for
advertising, publication, or promotional purposes.
Citation of trade names does not constitute an
official endorsement or approval of the use of
such commercial products.**

Unclassified

SECURITY CLASSIFICATION OF THIS PAGE (When Data Entered)

REPORT DOCUMENTATION PAGE		READ INSTRUCTIONS BEFORE COMPLETING FORM
1. REPORT NUMBER Miscellaneous Paper SL-82-10	2. GOVT ACCESSION NO. AD-7120669	3. RECIPIENT'S CATALOG NUMBER
4. TITLE (and Subtitle) THE HEMSS 3T EXPERIMENT		5. TYPE OF REPORT & PERIOD COVERED Final report
		6. PERFORMING ORG. REPORT NUMBER
7. AUTHOR(s) Anthony A. Bombich		8. CONTRACT OR GRANT NUMBER(s)
9. PERFORMING ORGANIZATION NAME AND ADDRESS U. S. Army Engineer Waterways Experiment Station Structures Laboratory P. O. Box 631, Vicksburg, Miss. 39180		10. PROGRAM ELEMENT, PROJECT, TASK AREA & WORK UNIT NUMBERS DNA Subtask Y99QAXSD070
11. CONTROLLING OFFICE NAME AND ADDRESS Defense Nuclear Agency Washington, D. C. 20305		12. REPORT DATE July 1982
		13. NUMBER OF PAGES 67
14. MONITORING AGENCY NAME & ADDRESS (if different from Controlling Office)		15. SECURITY CLASS. (of this report) Unclassified
		15a. DECLASSIFICATION/DOWNGRADING SCHEDULE
16. DISTRIBUTION STATEMENT (of this Report) Approved for public release; distribution unlimited.		
17. DISTRIBUTION STATEMENT (of the abstract entered in Block 20, if different from Report)		
18. SUPPLEMENTARY NOTES Available from National Technical Information Service, 5285 Port Royal Road, Springfield, Va. 22151. This is CTIAC Report No. 57.		
19. KEY WORDS (Continue on reverse side if necessary and identify by block number)		
20. ABSTRACT (Continue on reverse side if necessary and identify by block number) This investigation was conducted in support of Phase III of the High- Explosive Model Structure Simulation (HEMSS) Program to evaluate the properties in compression of 2C4 grout when cured at high temperatures. The results of the investigation are to be used to validate: (a) standard laboratory compres- sion tests conducted on 2C4 grout cylinders taken during casting of large 2.13-m (7-ft) diameter HEMSS cylinders for earlier phases of the program, and (b) other properties of the grout used in stress calculations based on the (Continued)		

Unclassified

SECURITY CLASSIFICATION OF THIS PAGE(When Data Entered)

20. ABSTRACT (Continued)

documented data on 2C4 grout.

A grout cylinder designated HEMSS 3T was cast to simulate the field conditions of the HEMSS No. 3 cylinder cast in 1978. HEMSS 3T was a 2.13-m (7-ft) diameter, 1.09-m (43-in.) high cylinder insulated on top and bottom to simulate the thermal conditions of the 4.27-m (14-ft) high field-cast cylinders. Grout test cylinders were cast at the time of casting HEMSS 3T, and were cured in ovens based upon temperatures at two locations in HEMSS 3T. At one of these locations, 0.610 m (24 in.) from the center, the peak temperature of 95.5°C (204°F) was recorded. This compares with 102°C (215°F) recorded in the HEMSS No. 3 cylinder. At the second location, 0.914 m (36 in.) from the center, 79.4°C (175°F) was recorded. Cores were taken from HEMSS 3T at these locations. Compression tests (A series) on cast cylinders were conducted at 1, 2, 6, 13, and 28 days after placement. Longitudinal velocity tests were also conducted at the same times on both cast cylinders and the HEMSS 3T cylinder.

Two series of static tests (C and B series) including triaxial, uniaxial, hydrostatic, and unconfined compression were conducted on cores taken from the two locations, respectively, in HEMSS 3T at 7 and 14 days age. Dynamic triaxial compression tests (SD series) were conducted on grout cores from the same location as the C-series specimens; i.e., on cores 0.610 m (24 in.) from the center at 14 days age only.

Computer simulations of the temperature and thermal strain achieved in HEMSS 3T were also conducted.

As a result of this investigation, it was found that the HEMSS 3T cylinder successfully duplicated the conditions in the HEMSS No. 3 field-cast cylinder except for the slightly lower peak temperature. Generally, the measureable effects of high temperature on the grout properties were not significant. Large differences were found between measured and calculated strain values. Also, strains measured by two different strain gages were substantially different. These differences are attributed to differences in the coefficients of thermal expansion of the grout and the gages. Some fracturing or material degradation occurred near the periphery of the HEMSS 3T cylinders which was attributed to the thermal restraint effects of the corrugated steel culvert used as the forms. It is recommended that lubricated forms rather than corrugated culverts be used for the outer forms.

11

Unclassified

SECURITY CLASSIFICATION OF THIS PAGE(When Data Entered)

Contents

	<u>Page</u>
Preface	1
Conversion Factors, Non-SI to SI (Metric) Units of Measurement	3
Introduction	4
Objective	4
Grout Specimens	4
Temperature Measurements	7
Strain Measurements	8
Tests of HEMSS 3T Grout	9
Longitudinal Ultrasonic Velocity in HEMSS 3T	10
Compression Tests of HEMSS 3T Cores	11
Temperature and Thermal Strain Simulations	13
Temperature simulation	13
Thermal strain computation	14
Discussion and Conclusions	14
References	17
Tables 1-9	
Figures 1-29	

Conversion Factors, Non-SI to SI (Metric)
Units of Measurement

Non-SI units of measurement used in this report can be converted to SI (metric) units as follows:

<u>Multiply</u>	<u>By</u>	<u>To Obtain</u>
bars	100,000	pascals
British thermal unit (International table) · feet per hour · square foot · degree Fahrenheit	1.730735	watts per metre · Kelvin
British thermal units (International table) per pound (mass) · degree Fahrenheit	4,186.8	joules per kilogram · Kelvin
calories (International table) per gram	4,186.8	joules per kilogram
cubic feet per minute	0.0004719474	cubic metres per second
Fahrenheit degrees	5/9	Celsius degrees or Kelvins*
feet	0.3048	metres
feet per second	0.3048	metres per second
inches	0.0254	metres
inches per inch per degree Fahrenheit	5/9	metres per metre per Kelvin
pounds (force) per square inch	0.006894757	megapascals
pounds (force) per square inch	6,894.757	pascals
pounds (force) per square inch per minute	114.9126167	pascals per second
pounds (mass) per cubic foot	16.01846	kilograms per cubic metre
square feet per hour	0.0000258064	square metres per second

* To obtain Celsius (C) temperature readings from Fahrenheit (F) readings, use the following formula: $C = (5/9)(F - 32)$. To obtain Kelvin (K) readings, use:
 $K = (5/9)(F - 32) + 273.15$.

THE HEMSS 3T EXPERIMENT

Introduction

1. The staff of the Structures Laboratory (SL) of the U. S. Army Engineer Waterways Experiment Station (WES) conducted a program in support of Phase III of the High-Explosive Model Structure Simulation (HEMSS) Program to evaluate the properties in compression of 2C4 grout when cured at high temperature.

2. During earlier phases of the program, conducted by Merritt CASES, Inc., intermediate-scale cylindrical test beds were cast from 2C4 grout. The dimensions of the test beds were 2.13 m (7 ft)* in outer diameter, 0.30 m (1 ft) in inner diameter, and 4.27 m (14 ft) in height. Three test beds were cast in 1977 and 1978 designated HEMSS 1, HEMSS 2, and HEMSS 3. Heat of hydration of cement resulted in measured peak temperatures of 108°C (226°F) and 128°C (262°F) for HEMSS 1 and HEMSS 2, respectively.

3. In 1978 a thermal analysis was conducted at WES¹ to evaluate HEMSS 1 and HEMSS 2, to assist in reducing temperatures in HEMSS 3, and to predict temperature rise and potentially damaging thermal strains in larger scale test beds. As a result of the WES investigation, peak temperatures were reduced to 102°C (215°F) in HEMSS 3. It was also found that higher temperatures and potentially damaging thermal strains would be probable in the larger scale 3.66- and 6.10-m (12- and 20-ft) diameter test beds then being contemplated. It was also suspected that the properties of grout curing at temperatures near or above 100°C (212°F) may differ from those obtained from tests of the grout cured at lower temperatures.

Objective

4. The objective of the study at WES in support of Phase III was to conduct static and dynamic tests of 2C4 grout cured at the elevated temperatures experienced in the HEMSS test beds. These data are to be used to validate standard laboratory compression tests² conducted prior to the HEMSS field tests and used in stress wave calculations.

Grout Specimens

5. The program included casting a test bed of the same material as used

* A table of factors for converting non-SI units of measurement to SI (metric) units is presented on page 3.

in the field in the Concrete Technology Division laboratory at WES from which specimens were cored for testing. This bed, designated HEMSS 3T, had the same inner and outer diameters as previous intermediate-scale beds but was only 1.06 m (3.5 ft) in height. The top and bottom surfaces were heavily insulated with urethane foam to simulate the thermal environment of full-height test beds. Thermal conditions were maintained to match as closely as possible the measured internal temperatures of HEMSS 3 cast in August 1978. The center cavity was ventilated with air from a 25.5-cu m/min (900-cu ft/min) fan. The outer surface (perimeter), consisting of a 2.13-m (7-ft) diameter steel culvert, was insulated with 0.038 m (1.5 in.) of fiber glass duct insulation for two short periods of time within the first two days after placement in order to maintain surface temperature near those measured in HEMSS3.

6. HEMSS 3T was instrumented with 37 thermocouples to measure temperatures in the grout mass, inner cavity forced air, laboratory air, and temperature in the top and bottom insulation. Figure 1 is an axisymmetric diagram of HEMSS 3T including the vertical layout of thermocouples. Table 1 lists the actual locations of thermocouples in the experiment.

7. HEMSS 3T also contained 12 internal strain gages placed at midheight of the grout mass. Strain gages consisted of seven WES-designed, low-modulus linear variable differential transformer (LVDT) gages, two internal Ailtech gages placed horizontally in the tangential direction, and three LVDT gages placed horizontally in the radial direction and spaced across the radius of the cylinder. Strain gage locations are shown in Figure 2 and listed in Table 2. The LVDT gages³ designed to measure strains in concrete or grout soon after placement, respond much earlier than the stiffer Ailtech gages. Measurement of strains in grout beginning immediately after placement is difficult when a large temperature change occurs simultaneously with thermal strain; the instantaneous coefficient of thermal expansion of the grout cannot be easily determined. Two types of strain gages were used to assist in the analysis of the strains and for cross comparison.

8. Thirty-two cylinders, 0.152- by 0.305-m, (6- by 12-in.) were cast and cured in three temperature environments as follows.

- a. Ten cylinders at the standard cure (A-series) used in all previous testing of the grout.
- b. Eleven cylinders at the medium temperature cure (B-series) which was specified to follow the temperature history in HEMSS 3T at a location reaching 79.4°C (175°F), and
- c. Eleven cylinders at the high temperature cure (C-series) which was specified to follow the temperature history in HEMSS 3T at the peak temperature location which reached 95.5°C (204°F).

9. The A-series cylinders were sealed and cured in water at the temperature environment of the standard cure. It was determined that the temperature environments specified for the B- and C-series cylinders required more rapid temperature change response, thus, they were lightly insulated and cured in variable temperature ovens. One cylinder in each of the B- and C-series was cast with an LVDT strain gage and thermocouple installed internally. No thermal strains were expected in these cylinders due to the insulation; therefore, "apparent" strains measured were intended to be used to assist in temperature correction at two thermally comparable strain gage locations in HEMSS 3T. In tests conducted prior to the grout casting, it was determined that plastic cylinder molds used at WES capable of providing a good seal deformed or melted at the high temperatures expected. Thus, heavily waxed cardboard molds and thin steel lids were used. A gasket of silicon-base caulk was formed in the lid, pressed down on the cylinder mold, and heavily taped with duct tape.

10. Sufficient grout was cast in 0.102-m (2-in.) diameter molds to produce four smaller 0.051- by 0.102-m (2- by 4-in.) cylinders for each of the B- and C-series environments. These cylinders were cast in split PVC pipes sealed with wax and heavily taped and also lightly insulated to eliminate any possibility of thermal strain.

11. Constituent materials for the grout mixture were obtained from the same sources in California as were used in the HEMSS field tests. The grout was mixed and pumped in one batch on 9 May 1979 with equipment similar to that used in the field tests. The grout was in place within 0.3 hr and had a measured unit weight of 2.176 g/cu cm (135.8 lb/cu ft). Table 3 defines the sequence of events for the entire experiment. Perimeter insulation was removed to coincide with the surface reaching approximately the same initial peak temperature measured in HEMSS 3 and was reinstalled for a 12 hr period after the surface temperature began to drop below the general surface temperature cooling trend measured in HEMSS 3. Forced air cooling of the center cavity was maintained for the initial five days after placement except for several hours on the fourth day (Sunday, 13 May 1979) when the fan failed.

12. Several related events occurred which prevented total success in the experiments. The seal failed on many of the 0.152- by 0.305-m (6- by 12-in.) cast cylinders in the B- and C-series environments and from vials of cement paste stored on the upper grout surface of HEMSS 3T. The paste was used for determination of heat of hydration at high temperature. It was concluded that vapor pressure caused by the high temperatures forced the seals to fail; thus all of the B- and C-series tests on 0.152- by 0.305-m (6- by 12-in.) cylinders and heat of hydration tests conducted after one day were on dehydrated specimens.

Moisture loss also occurred in the specimens containing LVDT gages. Thus, the use of strain records from these specimens was of little value in correcting strain records for temperature in HEMSS 3T. Since failure of the seals occurred later, all tests conducted at an age of 1 day were valid, as were all tests of 0.051- by 0.102-m (2- by 4-in.) cast cylinders for which little or no moisture loss occurred probably because there was an overabundance of wax.

13. All unconfined compression tests of the larger cylinders included determination of modulus of elasticity and were performed regardless of moisture loss at ages of 1, 2, 6, 13, and 28 days. Unconfined compressive strength tests were conducted on the smaller cast cylinders at ages of 6 and 13 days. Longitudinal velocity tests were performed on each test specimen on the day tested. Results of all tests on cast cylinders are shown in Table 4.

14. Heat of hydration tests were conducted at an age of 1 day on cement paste stored in vials located on the upper surface of HEMSS 3T. The temperature at the time of removal of the vials was approximately 87.8°C (190°F) or only 7.8°C (14°F) below the peak temperature of 95.5°C (204°F) reached in HEMSS 3T. Little or no moisture loss was believed to have occurred in the paste tested at 1 day. Heat of hydration was 0.330 MJ/kg (79 cal/g) compared with values of 0.364 MJ/kg (87 cal/g) calculated during the 1978 WES analysis which was based upon a 14.4°C (26°F) higher temperature rise at 1 day and 0.184 MJ/kg (44 cal/g) for Type "G" cement cured at the standard storage temperature of 21.1°C (73°F). Results of the remaining heat of hydration tests, which experienced moisture loss, are not reported here. The 1-day results, however, do substantiate the conclusion reached in the earlier WES study that heat of hydration is nearly doubled at 1 day when cured at the high temperatures observed here.

Temperature Measurements

15. Of the 37 thermocouples installed to measure temperature, only 2 failed during the time of temperature monitoring, and even these were redundant gages. Figure 3 shows typical temperature histories at nine locations between the inner cavity and perimeter surface of HEMSS 3T at the midheight of grout. Figures 4a through 4g show temperature distribution in the HEMSS 3T experiment at several ages. As a result of being heavily insulated, the vertical difference between peak temperatures reached at a radius of 0.610 m (24 in.) at an age of 1 day is only 4.44°C (8°F) when comparing temperatures at midheight and points 0.051 m (2 in.) from the top and bottom surfaces. The vertical temperature differences at most other radii were even smaller, and all differences

decreased with increasing time after peak temperature was reached. Therefore, it was concluded that cored specimens at any given radius received the same thermal curing environment, regardless of their elevation, as long as they were selected no closer than about 0.203 m (8 in.) from the top or bottom surfaces of HEMSS 3T.

Strain Measurements

16. Strains were recorded from time of placement until 28 days after completion of casting. After an age of 14 days, changes in temperature and strain were small. It was concluded from all strain records that initial set occurred at approximately 3 hr and final set at 6 to 8 hr after placement. Figure 5 shows tangential strains recorded from seven LVDT gages initialized at 8 hr. Recorded strains are substantially higher than expected and are believed to consist of true thermal strain plus apparent strain resulting from differences in the coefficients of thermal expansion of the gages $3.33 \times 10^{-6}/^{\circ}\text{C}$ ($6 \times 10^{-6}/^{\circ}\text{F}$) and the grout. It is known that the coefficient of expansion of the grout changes as a function of age, especially at early age, and of temperature due to the large temperature change and high water content in the grout. Correction for thermal expansion coefficient differences between gages and grout were dependent upon the apparent strain records from the LVDT gages in the B- and C-series "stress-free" cast cylinders. Moisture loss in these cylinders caused shrinkage which prevented a legitimate correction of HEMSS 3T strain records for isolation of thermal strain alone. The B- and C-series "stress-free" strain tests can be repeated to remove the temperature and autogenous volume changes from the HEMSS 3T strain records since additional constituent materials for this grout remain. A method of sealing specimens will have to be devised for the high temperature cure.

17. Figure 6 shows the comparative tangential strain records of LVDT and Ailtech gages located at radii of 0.610 and 0.991 m (24 and 39 in.). The 0.991-m (39-in.) radii gages show relatively similar records. However, the LVDT gage shows substantially greater strain in compression at 1 day at a radius of 0.610 m (24 in.). Actually, the strain recorded from the LVDT gage is proportionately closer to the expected strain at this radius when compared to the magnitude of tensile strains recorded near the perimeter. It has been learned in other subsequent work at WES that the Ailtech gage does not respond well in compression in a weak matrix. The small diameter barrel of the Ailtech gages possibly experiences flexure which may affect output when compressive strains are applied too early, whereas in tension the barrel is axially stretched,

providing better results. This may be the case here because the grout matrix is weak at the time of maximum compression. Other than the early age difference, changes in recorded strain from these LVDT and Ailtech gages are nearly identical after an age of 4 days.

18. Figure 7 shows radial strains recorded from the three radial LVDT gages. Again, these records have been started at 8 hr assuming zero-strain but have no other corrections made.

Tests of HEMSS 3T Grout

19. Compression tests of NX-size grout cores from HEMSS 3T were conducted in three series. Two of the test series were conducted at 7- and 14-days nominal age on specimens designated as C-series from the 95.5°C (204°F) and the B-series from the lower 79.4°C (175°F) peak temperature locations in HEMSS 3T. The radii of these coring locations were 0.610 and 0.914 m (24 and 36 in.), respectively. All tests were in static compression. The third series of tests, referred to as the SD series, was conducted on specimens from the high temperature 95.5°C (204°F) location only at 14-days nominal age and included static and dynamic triaxial compression tests only.

20. Figures 8a through 8e show the core logs and location of test specimens within the cores for all tests conducted. The length of the core barrel permitted cores as long as 0.406 m (16 in.) to be taken. Core sections taken from the 0.914-m (36-in.) radius did not break normal to the axis of the core barrel, especially in the 14-day borings, and the lengths were generally less than 0.406 m (16 in.). The difficulty in obtaining cores from this radius is indicated by the need for four holes, compared to three holes at the 0.610-m (24-in.) radius, in order to obtain the required number of usable test specimens. Although cracks were not observable to the eye, numerous specimens in the B-series broke during handling. Based upon the orientation of breaks in B-series cores, it is presumed that the differential cooling of nearly 33.3°C (60°F) that occurred between grout at the 0.610-m (24-in.) radius and that at the perimeter caused microfracturing to begin near the perimeter. The corrugated steel culvert probably restrained the outer surface of the grout from shrinking as the specimen cooled, contributing to microfracturing in patterns resembling concentric conical surfaces that became increasingly flatter with increasing depth. The cores drilled for the 14-day tests nearer to the perimeter showed a greater tendency to fracture than the cores drilled for the 7-day

tests. Visible cracks were not observed on the surface.

Longitudinal Ultrasonic Velocity in HEMSS 3T

21. Longitudinal ultrasonic velocity was measured at three radii in HEMSS 3T at ages of 1, 2, 6, and 13 days. Provision for making these measurements were made by coring 0.076-m (3-in.) diameter holes through the two thicknesses of 0.019-m (0.75-in.) plywood deck at radii of 0.61, 0.81, and 0.98 m (24, 32, and 39 in.) prior to casting grout. The holes were covered with thin sheet metal after the drilled wooden plugs were replaced. During each test a small section of the top and bottom surface insulation and the wooden plugs were removed. Velocity transducers were then positioned sequentially at each radii and longitudinal velocity through the entire height of HEMSS 3T obtained. The wooden plugs and insulation were then replaced to avoid undesired heat loss. The following table lists the longitudinal velocities obtained.

Radius m (in.)	Longitudinal Velocity - km/s (fps)			
	1 day	2 days	6 days	13 days
0.61 (24)	2.60 (8540)	2.74 (8980)	2.82 (9260)	2.84 (9335)
0.81 (32)	2.60 (8520)	2.73 (8960)	2.76 (9050)	2.72 (8940)
0.99 (39)	2.50 (8190)	2.57 (8440)	2.65 (8700)	2.64 (8660)

22. Similar longitudinal velocity tests were also performed on each NX-size cored specimen tested in the study. Each specimen was tested immediately after being surface ground on the same day it was cored. The individual velocities are included in Tables 4 through 7 where complete, individual test results are reported. The following table contains average longitudinal velocity measurements for specimens at all depths from 0.61- and 0.91-m (24- and 36-in.) radii for the 7- and 14-day test series.

Radius m (in.)	Longitudinal Velocity - km/s (fps)	
	7 Days	14 Days
0.61 (24) (C-series)	2.92 (9590)	2.93 (9610)
0.91 (36) (B-series)	2.92 (9570)	2.88 (9460)

23. Comparisons between the averages of velocities from individual small specimens and the measurements from large castings are typical of past experience

at WES. Longer path length invariably reduces velocity. Nevertheless, the reduction in longitudinal velocity at radii greater than or equal to 0.81 m (32 in.) between nominal ages of 7 and 14 days is further evidence that microfracturing occurred near the periphery of HEMSS 3T. Comparatively, during the same time span velocities at a radius of 0.61 m (24 in.) increased slightly; thus, if microfracturing has occurred at a radius of 0.61 m (24 in.), it has not affected the material enough to reduce longitudinal velocity.

Compression Tests of HEMSS 3T Cores

24. Several small test specimens were instrumented with two pairs of diametrically opposed bonded strain gages for measurement of axial and lateral strain. Specimens tested in the B- and C-series were nominally 0.099 m (3.90 in.) in length. Those tested in the SD-series were nominally 0.127 m (5 in.) in length. All specimens were cut to desired length, surface ground, and then sealed to preserve as-drilled moisture content. Strain gages were installed within "windows" of removed sealing material.

25. Static triaxial tests were originally specified to be conducted at confining pressures of 50, 100, and 150 MPa (0.5, 1.0, and 1.5 kbars). The first test conducted at 150 MPa (1.5 kbars) caused failure of one or more of the high-pressure connectors used to pass the strain gage leads through the pressure chamber wall. The connectors are rated for pressures of at least 275 MPa (2.75 kbars), but they had failed on several occasions on other programs at lower pressures. Although spare connectors were in stock to replace the entire set several times completely, the time required to change a set was too long to allow completion near the critical dates of the four series of tests (7 and 14 days at both locations) if additional failures occurred. Therefore, after consultation with Merritt CASES, Inc., the decision was made to delete all tests greater than 100 MPa (1.0 kbar) except for the last planned triaxial test to be attempted at 150 MPa (1.5 kbar). This was the only way to guarantee that the testing would proceed on schedule. In order that at least three tests be conducted in each triaxial test series, a test at 25 MPa (0.25 kbar) was conducted in place of the deleted 150 MPa (1.5 kbar) triaxial tests. Uniaxial and hydrostatic compression tests were initially requested to be conducted at 300 MPa (3.0 kbar). Due to the pressure chamber problems, these tests were also conducted to 100 MPa (1.0 kbar). No further difficulties were encountered except that severe leakage did occur on the final triaxial test at 150 MPa (1.5 kbar), but it was not so severe as to endanger the success of the test.

26. The 7-day static test series was actually conducted at ages of 7-9

days and the 14-day static test series was actually conducted at ages of 14 and 15 days.

27. Several more unconfined compression tests were conducted than planned because the results were lower than expected. In general the specimens from the B-series (0.91-m (36-in.) radius) showed greater variation in compressive strength, especially in the 14-day tests. This is thought to be the result of increasing microfracturing, which did not seem to affect the other compression tests conducted under three-dimensional confinement. Figure 9 is a graphic representation of results of all unconfined compression tests conducted.

28. Table 5 gives the results of all unconfined compressive strength tests on cored specimens. Also included are values of modulus of elasticity and Poisson's ratio for tests conducted on strain-gaged specimens. Longitudinal velocity tests were conducted on each specimen after completion of surface grinding. Shear velocity measurements were made on selected specimens only for the 14-day test series. Since the shear crystals are physically bonded to the specimens, there was danger of damaging the specimens when the crystals were removed.

29. The SD-series triaxial compression tests were conducted at the Geomechanics Division of the SL. Two static and five dynamic triaxial compression tests were conducted between ages of 12 and 15 days. Confining pressures were 3.7 and 7 MPa (0.037 and 0.07 kbar) in the static tests and 3.7 to 40 MPa (0.037 to 0.4 kbar) in the dynamic tests. One static test and three dynamic tests were conducted on strain-gaged specimens. All tests included an externally-mounted film potentiometer to assist in defining failure.

30. Table 6 gives a summary of all compression tests conducted on C-series specimens from the 95.5°C (204°F) location. Note that the lowest confining pressure triaxial test in this group at 14 days was conducted at 14 MPa (0.14 kbar) (2000 psi) to permit some comparison with the 7-MPa (0.07-kbar) test conducted at Geomechanics Division in the SD-series. Table 7 gives a summary of all compression tests conducted on B-series specimens from the 79.4°C (175°F) location. An extra triaxial test was conducted at a confining pressure of 72.4 MPa (0.724 kbar) in the 14-day series. In both Tables 6 and 7, unconfined compressive strength results are the averages of the three highest values obtained in each series and should be more representative of the true value; that is, these values are assured to be least affected by any microfracturing or other physical defects in the cored specimens. Table 8 contains a summary of the static and dynamic triaxial tests in the SD-series (same location as C-series) at 14 days. Water contents were not determined because the specimens are contaminated during testing.

31. Table 9 is a summary of the physical and mechanical properties of

2C4 grout compiled during this study. Also included for comparison are the values reported in Appendix A of the report by Cizek and Florence² for 2C4 grout properties exposed to the standard cure cycle.

32. Figures 10 through 13 show stress difference versus axial and lateral volume change for the B- and C-series static triaxial tests. Figures 14a and 14b show stress difference versus axial strain and stress difference versus principal strain difference for the one static and three dynamic tests, strain-gaged in the SD-series. Figure 15 shows the stress difference versus mean normal stress relationship for SD-series triaxial tests. Figures 16 through 18 show mean normal stress versus volume change for the hydrostatic phase of all triaxial compression tests conducted on strain-gaged specimens. In Figure 18 for the SD-series tests, specimen SD2.3B was subjected to dynamic hydrostatic loading and unloading then reloaded as a complete triaxial compression test. The unloading record from the initial hydrostatic loading was lost. Density of the specimen at the beginning of the triaxial test (SD2.3B(2)) was 2.21 gm/cu cm. No explanation has been found for the lower stiffness of the second hydrostatic loading. Figure 20 is the stress difference versus confining pressure relationships for all triaxial tests.

33. Figure 20 shows mean normal stress versus volume change for B- and C-series hydrostatic compression tests. Figure 21 shows stress difference versus confining pressure relationships for B- and C-series uniaxial compression tests. Figure 22 shows mean normal stress versus volume change in the B- and C-series uniaxial compression tests.

Temperature and Thermal Strain Simulations

34. A finite-element thermal analysis by Wilson⁴ of the HEMSS 3T experiment was conducted. The finite-element model shown in Figure 23 represents a one-fourth section horizontal cut. An axisymmetric simulation would have been beneficial except that the computer program does not as yet have this type element. The evaluation was, therefore, similar to that conducted at WES in 1978.

35. Temperature simulation. Some heat was assumed to be lost vertically through the top and bottom surfaces of HEMSS 3T, contributing to a reduction in peak temperature of 6.1°C (11°F) in HEMSS 3T when compared with that in the HEMSS 3 field test bed. To account for the peak temperature reduction, the adiabatic temperature rise used as input data and formulated in the earlier study was reduced by approximately this same amount (Figure 24). Measured air temperature curves for the inner cavity and laboratory air shown in Figure 25 were used as the exposure conditions on the inner and outer diameter surfaces,

respectively. Inner-cavity forced air velocity of 8.53 m/s (28 fps) was measured and the circulation velocity of the laboratory air was estimated to be 0.61 m/s (2 fps). These values were incorporated into the surface heat transfer coefficient boundary conditions. Values of specific heat and thermal conductivity were the same as used previously or 1457 J/kg (0.348 Btu/lb·°F) and 1.305 W/m·K (0.754 Btu·ft/hr·ft²·°F), respectively. Perimeter insulation equivalent to 0.038 m (1.5 in.) of fiber glass insulation was simulated as a change in surface heat transfer coefficient coincident with actual installation and removal times. Figure 26 shows the results of the temperature calculation simulation of HEMSS 3T. Computed temperature histories are very close to measured values, thus, validating the procedure.

36. Thermal strain computation. Thermal strains computed using the finite-element program by Sandhu⁵ were based upon the thermal loads represented by the computed temperature distribution histories for HEMSS 3T. The initial temperature distribution after which differential temperature change causes thermal strain is referred to as stress-free temperature and was computed at 8 hr after placement of grout for each element in the model. Other input included Poisson's ratio equal to 0.23 and an assumed constant coefficient of thermal expansion of $3.33 \times 10^{-6}/^{\circ}\text{C}$ ($6 \times 10^{-6}/^{\circ}\text{F}$). The modulus of elasticity versus age relationship used is shown in Figure 27 and is based upon the 1-day test values of cast cylinders and 7- and 14-day test values from HEMSS 3T cores in the B- and C-series. The increase is small from 1- to 14-days age.

37. Figures 28 and 29 show computed tangential and radial strains, respectively, for the same radii at which tangential and radial strains were measured. Although there are some detectable similarities when compared with the recorded values in Figures 5 and 7, the magnitudes are substantially lower for the computed values. As noted earlier, the gage records have not been corrected for coefficient of thermal expansion differences between gages and grout or for equal autogenous changes. Therefore, it is not possible to provide further discussion of calculated and measured values unless the tests are repeated in which instrumented "stress-free" grout cylinders are subjected to the same thermal histories as those at the gage locations for which correction is desired. Also, a test series is needed to determine coefficient of thermal expansion values of 2C4 grout considering both temperature and age dependence from time of setting and thereafter.

Discussion and Conclusions

38. In order to accomplish the goals of this study, it was imperative that the grout and the thermal conditions of cure in the WES test bed HEMSS 3T

matched closely that of previous efforts. The placement temperature of grout in HEMSS 3T was within 1°C (1.8°F) of the placement temperature of HEMSS 3 placed in California in 1978. The peak temperature of 95.5°C (204°F) was within the range of temperatures estimated before casting and 6.1°C (11°F) less than in HEMSS 3. Examination of the temperature distribution in HEMSS 3T showed that the initial temperature loss at the top and bottom surfaces was nearly equivalent to the heat required to warm the insulation to the equilibrium thermal gradient across it at the time that peak temperature was reached. Vertical heat loss after peak temperature was reached was very small due to the urethane insulation. For practical purposes the test bed underwent only horizontal heat loss and the grout at any radii experienced the same thermal curing environment.

39. Compressive strengths at an age of 14 days for cast cylinders exposed to the same curing conditions used in previous testing of 2C4 grout were 130 psi lower than the reported average value. Although longitudinal velocities and modulus of elasticity were also slightly lower than previously reported values, for practical purposes the grout was essentially duplicated.

40. Generally, the higher temperature cures at which the test specimens were subjected in this study did not produce substantially different properties when compared with reported values at the standard cure. Porosity was approximately 2 percent lower in this study. The degree of saturation measured was 93 to 94 percent compared with a reported value of 99 to 100 percent even though moisture was preserved in cored specimens during preparation. The lower saturation is probably a direct result of the higher temperature curing conditions. It is believed that the wet coring may have in fact added a small amount of water which may account for some of the variation in compressibility seen in hydrostatic compression test results. The speed of drilling for B-series cores was slowed because of the difficulty in obtaining usable specimen material; thus, exposure to drilling water was longer. This may be the cause of slightly higher average densities in that series.

41. Compressive strengths of cored specimens varied considerably and at an increasing rate with age, especially in the B-series tests. Although it was not proven decisively, it is believed that the differential temperature environment in HEMSS 3T caused microfracturing or some other material degradation, especially in the B-series specimens which became more severe with increasing age. This is substantiated by fracturing of cores during drilling and handling, which produced breaks that were generally angular with respect to the core axis, reduced longitudinal velocity with increasing age, and unusual failure modes during testing. Compressive tests of 0.051- by 0.102-m (2- by 4-in.) cast cylinders cured at the thermal environment of the B- and C-series specimen locations in HEMSS 3T produced were within the ranges of previously reported values. Therefore,

it is concluded that the lower compressive strengths seen in many of the cored specimens are not a result of the higher curing temperatures but a result of thermally induced stresses caused or aggravated by the corrugated steel culvert during differential cooling.

42. Modulus of elasticity from unconfined compression tests of cored specimens averaging 9.24 Gpa (1.34×10^6 psi) showed the largest difference of any property when compared with the previously reported values of 18.2 Gpa (2.64×10^6 psi). Poisson's ratio of 0.23 was also lower than the previously reported value of 0.29. These lower values may also reflect microfracturing or other degradation. The remaining tests, including triaxial, uniaxial, and hydrostatic compression, did not show substantial difference when compared with the limited amount of previously reported data. Details of all phases of the test program which produced the reported values are not available. Further comparisons cannot be justified because variations in the techniques used could account for the differences in results. Shear strengths of specimens tested in dynamic triaxial compression were 20 to 25 percent higher than those obtained during static compression.

43. This study did show that considerable efforts are needed in refining in situ measurement of thermal strain in grout beginning at placement and thereafter when large temperature change occurs. When the seals failed on the instrumented cylinders which were to be used for isolating thermal strain from the HEMSS 3T strain gages, the corrections for differences in thermal coefficient of expansion between the grout and strain gages could not be made. It was believed from the outset of this study that the coefficient of thermal expansion of 2C4 grout cured in the thermal conditions of the HEMSS test beds was a function of age and temperature. A test program to isolate this variability was not possible within the monetary constraints of the study. It is recommended that these relationships be determined. A sufficient amount of constituent materials for grout used in HEMSS 3T does remain to perform this work. In fact if the "stress-free" cylinder tests of this study are successfully repeated, the strain records from HEMSS 3T can yet be corrected to isolate pure thermal strain. Unless corrected strains are obtained, computation of thermal strain in 2C4 grout placed in mass quantities cannot be validated and the consequences of casting 2C4 in larger volumes cannot be firmly established. Since it was concluded that temperature correction of strains measured in HEMSS 3T was needed, further numerical evaluations beyond the single run made in this program would not have been meaningful.

44. In the event that 2C4 grout is continued to be used in the HEMSS program, it is recommended that smooth-surface, lubricated forms be used instead of corrugated steel culverts, to reduce restraint that may produce cracking in the grout during the cooling period.

References

1. Bombich, A. A., "Thermal Studies of HEMSS Cylindrical Test Beds Containing SRI-RMG-2C4 Grout," Miscellaneous Paper SL-82-9 (CTIAC Report No. 56), Jul 1982, U. S. Army Engineer Waterways Experiment Station, Vicksburg, Miss.
2. Cizek, J. C. and Florence, A. L., "Laboratory Studies of Containment in Underground Nuclear Tests," Report No. DNA 0000F, Jan 1979, SRI International, Menlo Park, Calif.
3. Alexander, A. M., "A Low-Modulus Internal Concrete Strain Meter," Miscellaneous Paper C-74-9, Jun 1974, U. S. Army Engineer Waterways Experiment Station, Vicksburg, Miss.
4. Wilson, E. L., "The Determination of Temperatures Within Mass Concrete Structures," Report No. 68-17, Dec 1968, Structural Engineering Laboratory, University of California, Berkeley, Calif.
5. Sandhu, R. S., Wilson, E. L., and Raphael, J. M., "Two-Dimensional Stress Analysis with Incremental Construction and Creep," Report No. 67-34, Dec 1967, Structural Engineering Laboratory, University of California, Berkeley, Calif.

Table 1
Temperature Measurement (Thermocouple)
Locations in HEMSS 3T

<u>Radius</u> <u>m (in.)</u>	<u>Depth</u> <u>m (in.)</u>	<u>Number of Gages</u> <u>at Radius</u>
0.610 (24)	1.092 (43)	1
0.203 (8)	1.041 (41)	1
0.991 (24)	1.041 (41)	1
0.203 (39)	1.041 (41)	1
0.457 (8)	0.889 (35)	1
0.762 (18)	0.889 (35)	1
0.991 (30)	0.889 (35)	1
0.152 (39)	0.889 (35)	1
0.203 (6)	0.559 (22)	1
0.305 (8)	0.559 (22)	2
0.457 (12)	0.559 (22)	2
0.610 (24)	0.559 (22)	3
0.762 (30)	0.559 (22)	1
0.914 (36)	0.559 (22)	3
0.991 (39)	0.559 (22)	2
1.041 (41)	0.559 (22)	1
0.457 (18)	0.254 (10)	1
0.762 (30)	0.254 (10)	1
0.203 (8)	0.051 (2)	1
0.610 (24)	0.051 (2)	1
0.991 (39)	0.051 (2)	1
0.610 (24)	0.0 (0)	1

Additional Thermocouples Located:

(1) In air - laboratory air temp.	1
(2) In center cavity at depth of 0.559 m (22 in.), forced air temp.	1
(3) On top surface of cover insulation	1
(4) In support structure	4

Total Thermocouples 37

Table 2
Locations of 12 Internal Strain Gages in
HEMSS 3T at Depth of 0.559 m (22 in.)

<u>Radius</u> <u>m (in.)</u>	<u>Type</u> <u>Gage</u>	<u>Type Strain</u> <u>Measurement</u>
0.203 (8)	LVDT	Tangential
0.305 (12)	LVDT	Tangential
0.457 (18)	LVDT	Tangential
0.610 (24)	LVDT	Tangential
0.762 (30)	LVDT	Tangential
0.914 (36)	LVDT	Tangential
0.991 (39)	LVDT	Tangential
0.610 (24)	Ailtech	Tangential
0.991 (39)	Ailtech	Tangential
0.305 (12)	LVDT	Radial
0.610 (24)	LVDT	Radial
0.914 (36)	LVDT	Radial

Table 3
Chronology of Events for HEMSS 3T

<u>Day</u>	<u>Date</u>	<u>Time (hr)</u>	<u>Elapsed Time (days)</u>	<u>Event</u>
Wednesday	9 May 79	0940	-0.014	Grout placement begins.
		1000	0.000	Grout placement completed.
		1130	0.0625	Top and perimeter insulation in place. Forced air ventilation begins.
		1300	0.125	Initial set estimated.
		1800	0.333	Final set estimated. Perimeter insulation removed.
Thursday	10 May 79	1300	1.125	Peak temperature reached.
		1600	1.250	Perimeter (O.D.) insulation re-installed
Friday	11 May 79	0800	1.917	Perimeter insulation removed.
Sunday	13 May 79	0400	3.750	Forced air lost.
		1000	4.000	Forced air restored.
Monday	14 May 79	1000	5.000	Forced air ends. Drilling of 7-day cores begins.
Tuesday	15 May 79	1200	6.083	Drilling of 7-day cores ends.
Wednesday	16 May 79	0800	6.917	7-day test series begins.
Friday	18 May 79	0800	8.917	Drilling of 14-day cores for Geomechanics Division begins.
		1300	9.125	Drilling of 14-day cores ends.
Monday	21 May 79	1400	9.250	7-day test series ends.
		0800	11.917	Drilling of 14-day cores begins. 14-day test series begins at Geomechanics Division.
Tuesday	22 May 79	1200	13.083	Drilling of 14-day cores ends.
Wednesday	23 May 79	0800	13.917	14-day test series begins.
Thursday	24 May 79	1600	15.250	All 14-day tests end.
Friday	8 Jun 79	1000	28.000	Instrumentation monitoring in HEMSS 3T ends. 28-day compression tests made.

Table 4

Test Results - Cast 2C4 Grout Cylinders

Age	Series No.	Type Specimen	Type **	No. Tested	Compressive Strength		Modulus of Elasticity		Density g/cm ³	Long. Velocity km/s
					MPa	psi	GPa	x 10 ⁶ psi		
1	A	L		2	13.85	2010	9.93	1.44	2.17	2.76
	B	L		2	13.38	1940	9.17	1.33	2.17	2.59
	C	L		2	13.72	1990	8.63	1.26	2.17	2.58
2	A†	L		2	18.00	2610	11.17	1.62	2.18	2.99
	B†	L		2	16.00	2320	10.76	1.56	2.12	2.68
	B	L		2	17.17	2490	9.31	1.35	2.08	2.79
6	A†	L		2	23.10	3350	13.31	1.93	2.18	3.05
	B†	L		2	18.40	2670	11.17	1.62	2.07	2.72
	C	L		2	23.00	3360	9.31	1.35	2.05	2.88
13		S		2	22.20	3220	--	--	2.16	2.73
	C	S		2	23.30	3380	--	--	2.14	2.90
	A†	L		2	26.34	3820	15.44	2.24	2.17	2.99
28	B†	L		2	21.17	3070	10.82	1.57	2.06	2.71
	C†	L		2	23.86	3460	11.03	1.60	2.02	3.01
	B	S		2	24.30	3525	--	--	2.13	2.72
28	C	S		2	27.10	3930	--	--	2.16	2.92
	A†	L		2	27.37	3970	16.34	2.36	2.17	3.11
	B†	L		2	18.48	2680	11.85	1.72	2.03	2.95
	C	L		2	22.65	3285	10.41	1.51	1.98	2.88

* Series Key-Cast Cylinders

A - Standard cure - 48.9°C (120°F) peak temperature cure - immersed.

B - 93°C (200°F) peak temperature cure in oven.

C - 79.4°C (175°F) peak temperature cure in oven.

** L - 0.152- by 0.305-m (6- by 12-in.) cast cylinders.

S - 0.051- by 0.102-m (2- by 4-in.) cast cylinders.

NX - NX core, nominal diameter 0.0538 m (2.120 in.).

† Seal failed - moisture lost.

Table 5
Test Results of Cored 2C4 Grout Specimens

Age- Tested/ (Cored) (Days)	Specimen No.	Average Depth m	Density g/cm ³	Compressive Strength		Modulus of Elasticity		Poisson's Ratio	Long. Velocity km/s
				MPa	psi	GPa	x 10 ⁶ psi		
7 (5)	C1-2C	0.55	2.16	23.3	3380	9.58	1.39	0.22	2.95
8 (6)	B4-5B	0.86	2.17	21.4	3100	9.79	1.42	0.22	2.92
9 (5)	B1-4A	0.64	2.16	23.4	3390	10.07	1.46	0.22	2.97
9 (6)	B3-3B	0.90	2.16	23.4	3400	10.14	1.47	0.22	3.02
9 (5)	C3-3A	0.38	2.16	22.6	3280	10.20	1.48	0.22	2.82
9 (5)	C3-4A	0.76	2.17	23.3	3380	9.38	1.36	0.24	2.98
9 (9)	SDC1-1A	0.25	2.16	25.1	3640	--	--	--	2.91
9 (9)	SDC1-2A	0.58	2.16	20.9	3030	--	--	--	2.92
13 (9)	SDC1-1B	0.36	2.16	25.4	3690	--	--	--	2.98
13 (9)	SDC2-2	0.58	2.17	24.1	3500	--	--	--	2.93
14 (12)	B5-2	0.32	2.15	21.6	3130	8.48	1.23	0.23	2.87
14 (12)	B5-2	0.48	2.17	18.6	2700	9.51	1.38	0.22	2.78
15 (5)	B1-2A	0.35	2.17	23.1	3350	--	--	--	2.89
15 (5)	B4-3	0.47	2.16	21.0	3040	9.44	1.37	0.23	2.87
15 (5)	B6-4	0.68	2.16	17.7	2570	--	--	--	2.90
15 (12)	B7-3A	0.62	2.15	15.8	2290	--	--	--	--
15 (12)	B7-3C	0.83	2.18	25.0	3630	--	--	--	2.98
15 (12)	C4-3A	0.75	2.17	25.2	3660	8.69	1.26	0.22	2.91
15 (12)	C5-2C	0.51	2.18	22.3	3230	9.44	1.37	0.23	2.96
15 (12)	C5-3B	0.81	2.18	16.8	2430	--	--	--	2.92
15 (12)	C6-2B	0.43	2.17	26.1	3790	9.79	1.42	0.26	2.96
15 (9)	SDC1-3	0.89	2.18	24.6	3570	--	--	--	2.98
15 (9)	SDC3-1	0.22	2.17	25.9	3760	--	--	--	3.01

(Continued)

Table 5 (Concluded)

Age- Tested/ (Cored) (Days)	Specimen No.	Average Depth m	Density g/cm ³	Compressive Strength		Modulus of Elasticity		Poisson's Ratio	Long. Velocity km/s
				MPa	Psi	GPa	x 10 ⁶ psi		
28 (12)	B6-2T	0.22	2.16	22.1	3210	--	--	--	2.78
28 (12)	B5-4L	0.93	2.18	25.3	3660	--	--	--	2.86
28 (12)	B6-5L [†]	0.96	2.17	27.2	3940	--	--	--	2.98
28 (12)	B8-1T [†]	0.11	2.17	17.3	2510	--	--	--	--
28 (12)	C5-1T [†]	0.20	2.17	19.0	2750	--	--	--	2.94
28 (12)	C6-1T [†]	0.20	2.15	16.6	2410	--	--	--	2.90
28 (12)	C5-3L	0.91	2.18	20.1	2910	--	--	--	2.92
28 (12)	C6-3L	0.92	2.18	25.0	3630	--	--	--	2.91

* Core locations in HEMSS3T (by specimen No. prefix)

B - 0.91-m (36-in.) radius or 0.762 (30 in.) radially from inside diameter.

C - 0.61-m (24-in.) radius or 0.46 m (18 in.) radially from inside diameter.

SD - same as C, specimens cored for tests at WES-SL-Soil Dynamics Division

** Actual maximum depth - 1.10 m (43.5 in.).

† Results may not be characteristic of material. Location is near top surface.

NOTE: Longitudinal velocities shown with 28-days age tests were values obtained at 14 days.

Table 6

Summary of C-Series Compression Tests of 2C4 Grout

Specimens cored from HEMSS 3T experiment at radius = 0.61 m (24 in.).
Peak curing temperature = 95.5°C (204°F)

Specimen No.	Age (days)	Test *	Average Depth (m)	Density (g/cm ³)	Water Content By Wet Wt. (Percent)	Long. Velocity (km/s)	Maximum Confining Pressure σ_3 (MPa)	Maximum Axial Stress σ_1 (MPa)	Maximum Stress Difference $\sigma_1 - \sigma_3$ (MPa)	Maximum Volume Change (Percent)
C (AVG3)	7, 9, 9	UC	0.56	2.16	17.3	2.95	0.0	23.1	23.1	0.0
C2-3B	8	TX	0.48	2.16	17.2	2.90	25.0	57.9	37.9	0.460
C1-2A	7	TX	0.34	2.17	17.2	2.89	50.0	81.3	31.3	1.312
C1-2B	7	TX	0.45	2.17	17.4	2.91	100.0	134.7	34.7	1.632
C2-3A	7	TX	0.38	2.16	--	2.91	150.0	Test failed		2.305
C3-3B	8	HYD	0.48	2.17	16.9	2.82	100.0	100.0	0.0	2.144
C3-3C	9	UX	0.58	2.16	16.8	2.82	83.1	100.0	24.5	2.724
<u>14-Days Age Test Series</u>										
C (AVG3)	15, 15, 15	UC	0.56	2.18	16.7	2.94	0.0	25.8	25.8	0.0
C6-2C	15	TX	0.53	2.17	16.7	2.92	13.8	53.3	39.5	0.180
C4-2B	15	TX	0.41	2.18	17.2	2.94	50.0	87.4	37.4	1.810
C4-2C	15	TX	0.51	2.18	16.3	2.94	100.0	144.9	44.9	1.948
C6-3B	15	TX	0.82	2.18	16.7	2.88	150.0	200.3	50.3	2.615
C5-3A	15	HYD	0.71	2.17	16.9	2.94	100.0	100.0	0.0	2.272
C6-3A	15	UX	0.72	2.18	16.4	2.91	83.4	100.0	22.5	2.920

* Tests: UC - Unconfined Compression (values are average of 3 highest compressive strengths in test series).
TX - Triaxial Compression.

HYD - Hydrostatic Compression.

UX - Uniaxial Compression.

** Value is from hydrostatic or uniaxial compression.

Table 7

Summary of B-Series Compression Tests of 2C4 Grout

Specimens cored from HEMSS 3T experiment at radius = 0.91 m (36 in.).
Peak curing temperature = 79.4°C (175°F).

Specimen No.	Age (days)	Test *	Average Depth (m)	Density (g/cm ³)	Water Content By Wet Wt. (Percent)	Long. Velocity (km/s)	Maximum Confining Pressure σ_3 (MPa)	Maximum Axial Stress σ_1 (MPa)	Maximum Stress Difference $\sigma_1 - \sigma_3$ (MPa)	Maximum Volume Change (Percent)
B (Avg of 3)	8, 9, 9	UC	0.80	2.16	16.5	2.97	0.0	22.7	22.7	0.0
B3-3A	8	TX	0.80	2.17	17.2	2.96	25.0	57.7	32.7	0.420
B1-5A	8	TX	0.76	2.16	16.6	2.99	50.0	83.8	33.8	2.132
B2-4A	8	TX	0.76	2.16	16.8	3.03	100.0	132.2	32.1	1.512
B4-5A	9	HYD	0.76	2.17	16.9	2.98	100.0	100.0	0.0	1.724
B1-5B	9	UX	0.86	2.17	--	2.88	77.9	100.0	27.4	2.192
B (Avg of 3)	14, 15, 15	UC	0.50	2.17	17.5	2.91	0.0	23.2	23.2	0.0
B7-3B	14	TX	0.72	2.17	17.4	2.94	25.0	62.0	37.0	0.398
B6-5	14	TX	0.86	2.17	17.6	2.98	50.0	84.6	34.6	1.105
B6-3	15	TX	0.46	2.16	17.4	2.88	72.4	110.7	38.2	1.819
B5-4	14	TX	0.83	2.17	18.0	2.86	100.0	142.6	42.6	1.804
B8-4	15	HYD	0.73	2.17	17.5	2.86	100.0	100.0	0.0	1.56
B7-2	14	UX	0.34	2.17	17.5	2.78	86.2	100.0	25.8	2.640

* Tests: UC - Unconfined Compression (average of 3 highest compressive strengths in test series).
TX - Triaxial Compression.

HYD - Hydrostatic Compression.

UX - Uniaxial Compression.

** Value is from hydrostatic or uniaxial compression.

Table 8

Summary of SD-Series Triaxial Compression Tests

Specimens cored from HEMSS 3T experiment at radius = 0.61 m (24 in.).
Peak curing temperature = 95.5°C (204°F)

Specimen No.	Test Age (days)	Average Depth (m)	Density (g/cm ³)	Long. Velocity (km/s)	Type Test	Confining Pressure σ_3 (MPa)	Stress Difference $\sigma_1 - \sigma_3$ (MPa)	Maximum Volume Change (Percent)
SD2-1	12	0.32	2.16	2.92	Static	3.7	31.4	--
SD1-2	13	0.47	2.16	2.95	Static	7.0	38.0	0.16
SD2-2	12	0.46	2.17	3.03	Dynamic	3.7	40.6	--
SD3-1	14	0.33	2.15	2.90	Dynamic	6.8	47.5	0.12
SD3-2A	14	0.46	2.17	2.97	Dynamic	15.5	56.9**	0.36
SD3-2B	12	0.59	2.15	2.95	Dynamic	15.0	45.2	--
SD2-3(1) [†]	15	0.90	2.18	2.97	Dynamic	40.0	Hydro only	0.65
SD2-3(2)			2.21	--	Dynamic	40.0	46.3	1.20

* Maximum volume change during hydrostatic phase. If blank, not strain-gaged.

** Failure stress questionable.

[†] Specimen loaded and unloaded hydrostatically, then complete triaxial test run.

Table 9

Summary of 14-Day Test Results, 2C4 Grout

	Cores from HEMSS 3T		Standard Cure		Cast Cylinders*				Previous Studies
	B-Series SD & C Series		A-Series		B-Series		C-Series		
	NX Cores	NX Cores	SI	SI†	SI†	S2††	SI†	S2	
Specimen size	79.4 (175)	95.5 (204)	48.9 (120)	79.4 (175)	87.8 (190)	87.8 (190)	87.8 (190)	87.8 (190)	48.9 (120)
Max curing temperature °C(°F)	2.164	2.170	2.170	2.06	2.13	2.02	2.16	2.15	2.15
Density, g/cm ³ , as tested	1.820	1.824	--	--	--	--	--	1.75	1.75
dry	2.881	2.885	--	--	--	--	--	2.87	2.87
grain	36.8	36.8	--	--	--	--	--	39.0	39.0
Porosity, %	17.6	16.9	--	--	--	--	--	18.6	18.6
Moisture (by wet weight, %)	93.5	94.6	--	--	--	--	--	99-100	99-100
Saturation, %	2.88	2.95	2.92	2.71	2.72	3.01	2.92	3.29	3.29
Longitudinal velocity (km/sec)	1.66	1.64	--	--	--	--	--	1.82	1.82
Shear velocity (km/sec)	20.41±3.51	23.81±3.10	26.34	21.17	24.30	23.86	27.10	27.51	27.51
Unconf. compr. strength, Standard Deviation, MPa (psi)	(2960±466)	(3454±450)	(3820)	(3070)	(3525)	(3460)	(3930)	(3990)	(3990)
Modulus of elasticity, GPa (x 10 ⁶ psi)	9.30	9.17	15.44	10.82	--	11.03	--	18.20	18.20
(x 10 ⁶ psi)	(1.35)	(1.33)	(2.24)	(1.57)	--	(1.60)	--	(2.64)	(2.64)
Poisson's Ratio	0.227	0.237	--	--	--	--	--	0.28	0.28
Shear Angle, φ, radians (degrees)	0.0408	0.0454	--	--	--	--	--	0.0436	0.0436
(degrees)	(2.34)‡	(2.60)‡‡	--	--	--	--	--	(2.5)	(2.5)

* Specimen size key SI - 0.152- by 0.305-m (6- by 12-in.) cylinders; S2 - 0.051- by 0.102-m (2- by 4-in.) cylinders.

** From Reference 1.

† Seal failed - substantial moisture loss.

†† Slight moisture loss.

‡ Best fit of four tests.

‡‡ Best fit of six static tests.

HEMSS 3T EXPERIMENT - CAST 9 MAY 1979 AT USAEWES STRUCTURES LABORATORY

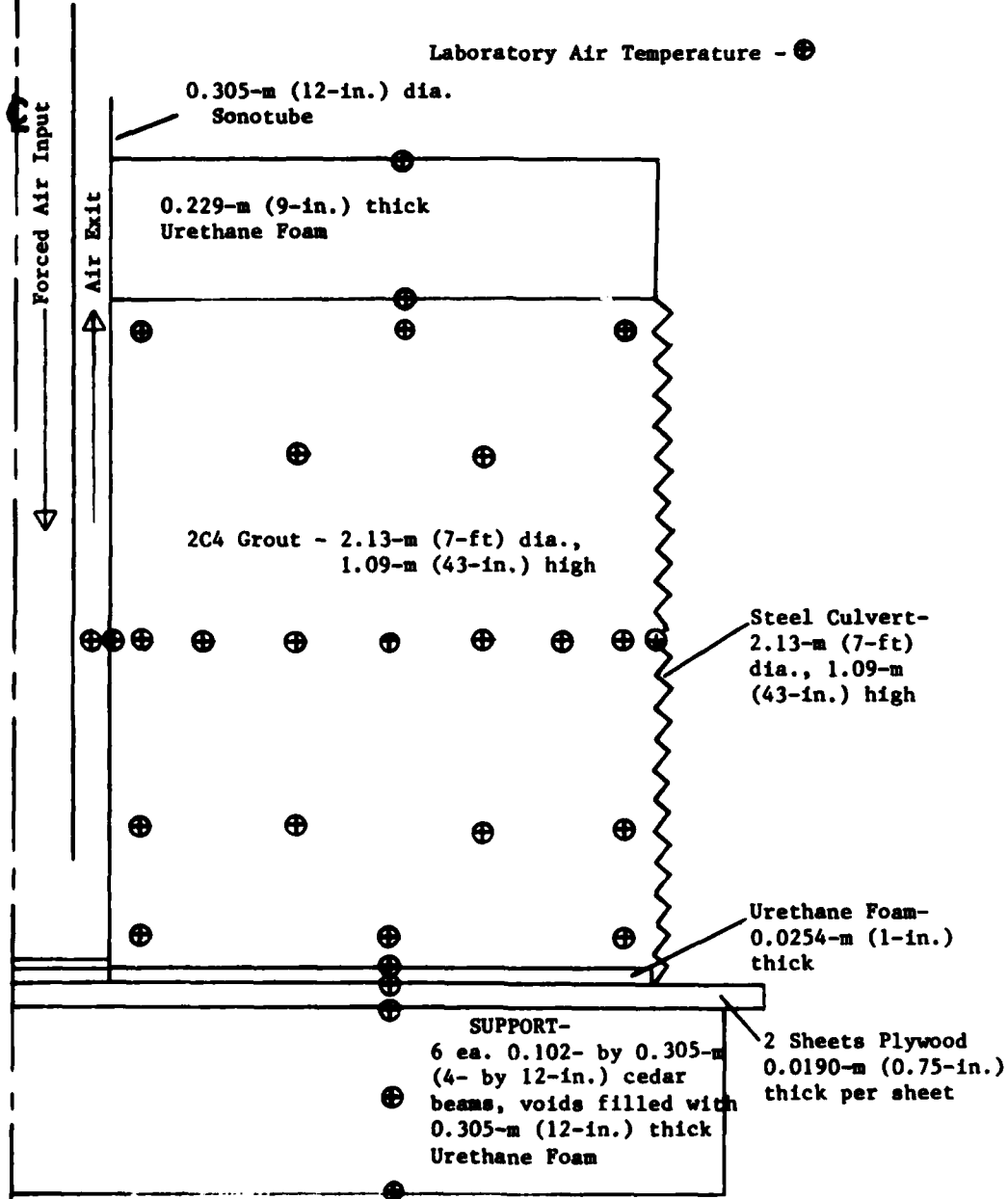


Figure 1 - Axisymmetric view of HEMSS 3T experiment with thermocouple locations indicated.

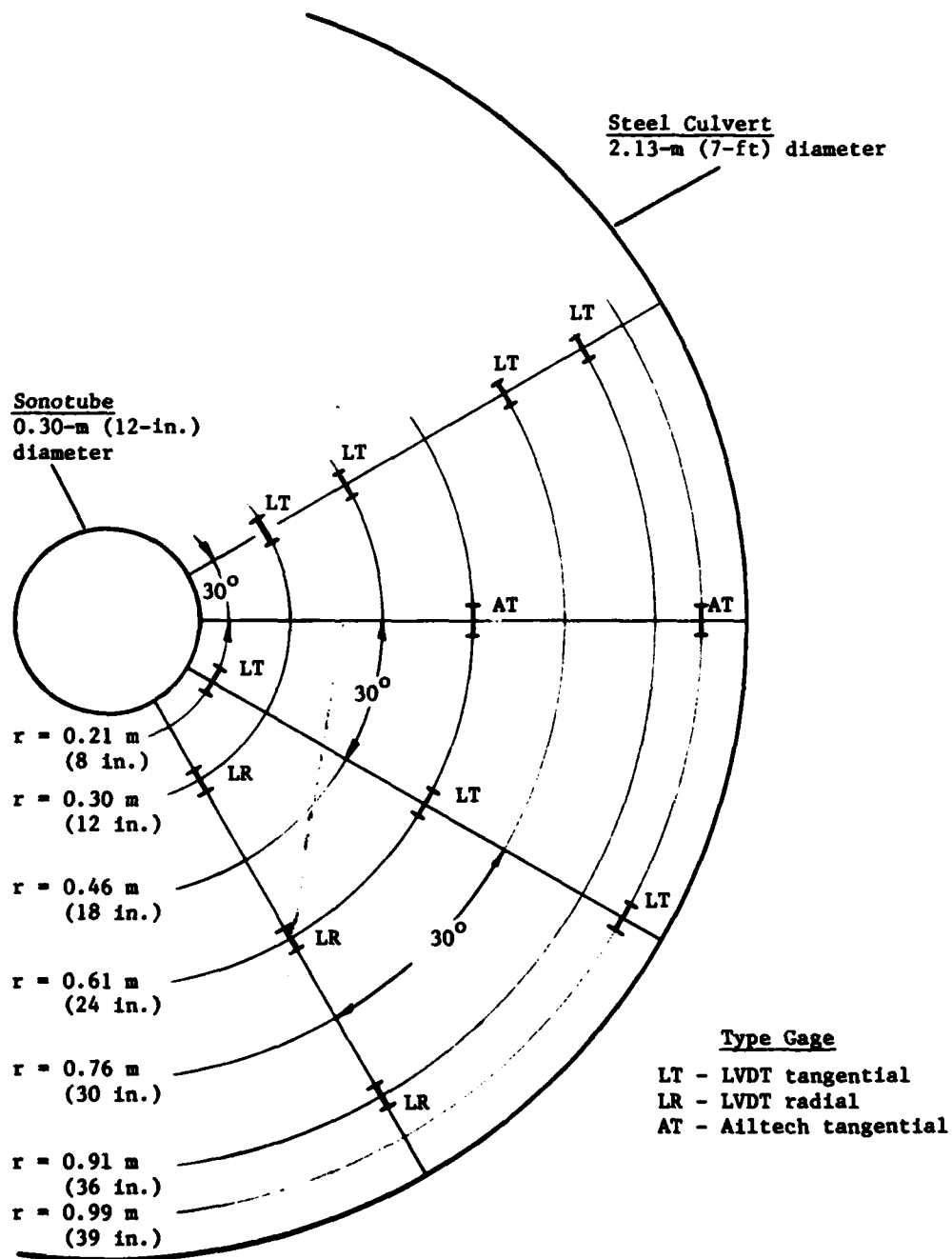


Figure 2 - Plan view of strain gages in HEMSS 3T at mid-height of grout.

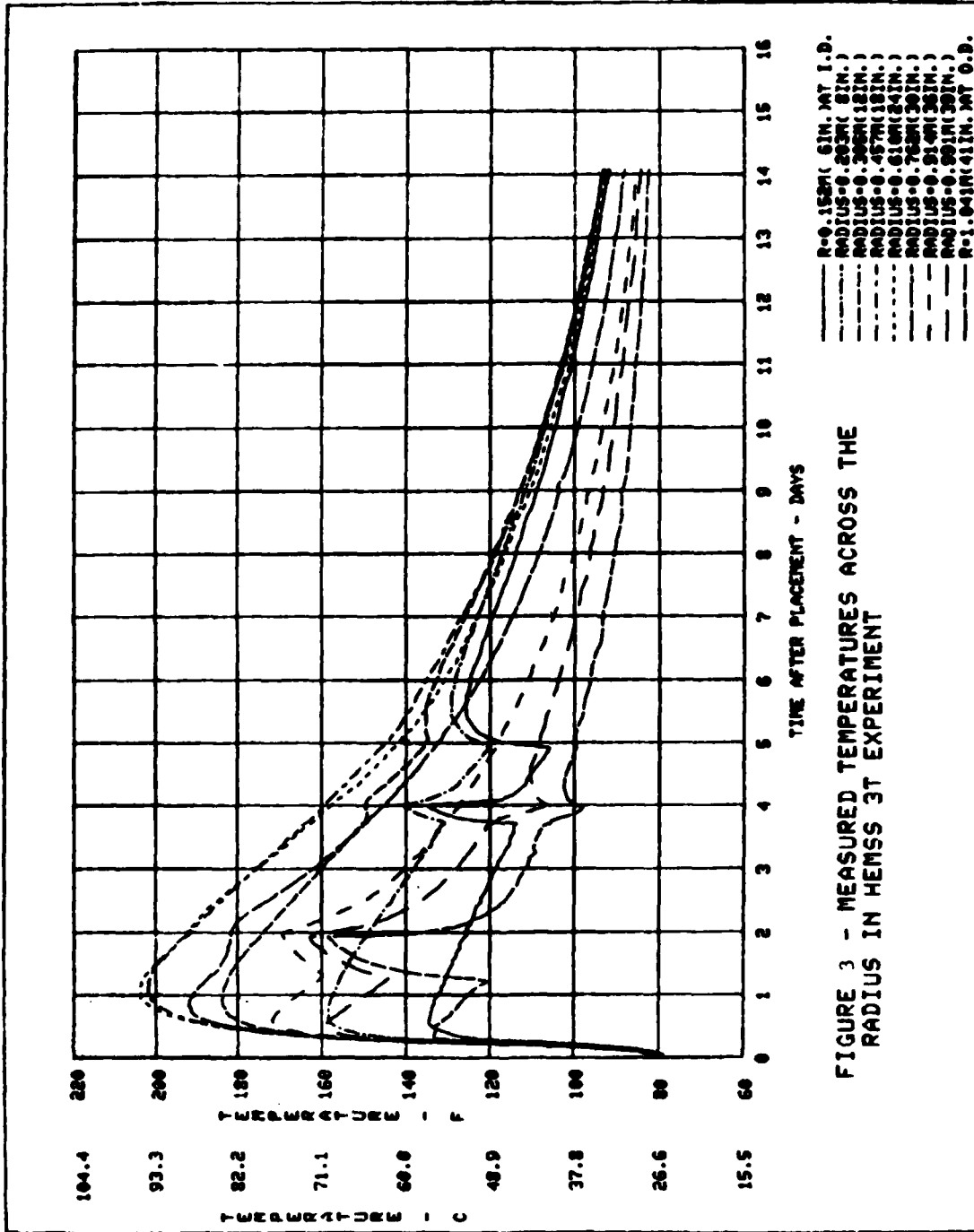


FIGURE 3 - MEASURED TEMPERATURES ACROSS THE
 RADIUS IN HEMSS 3T EXPERIMENT

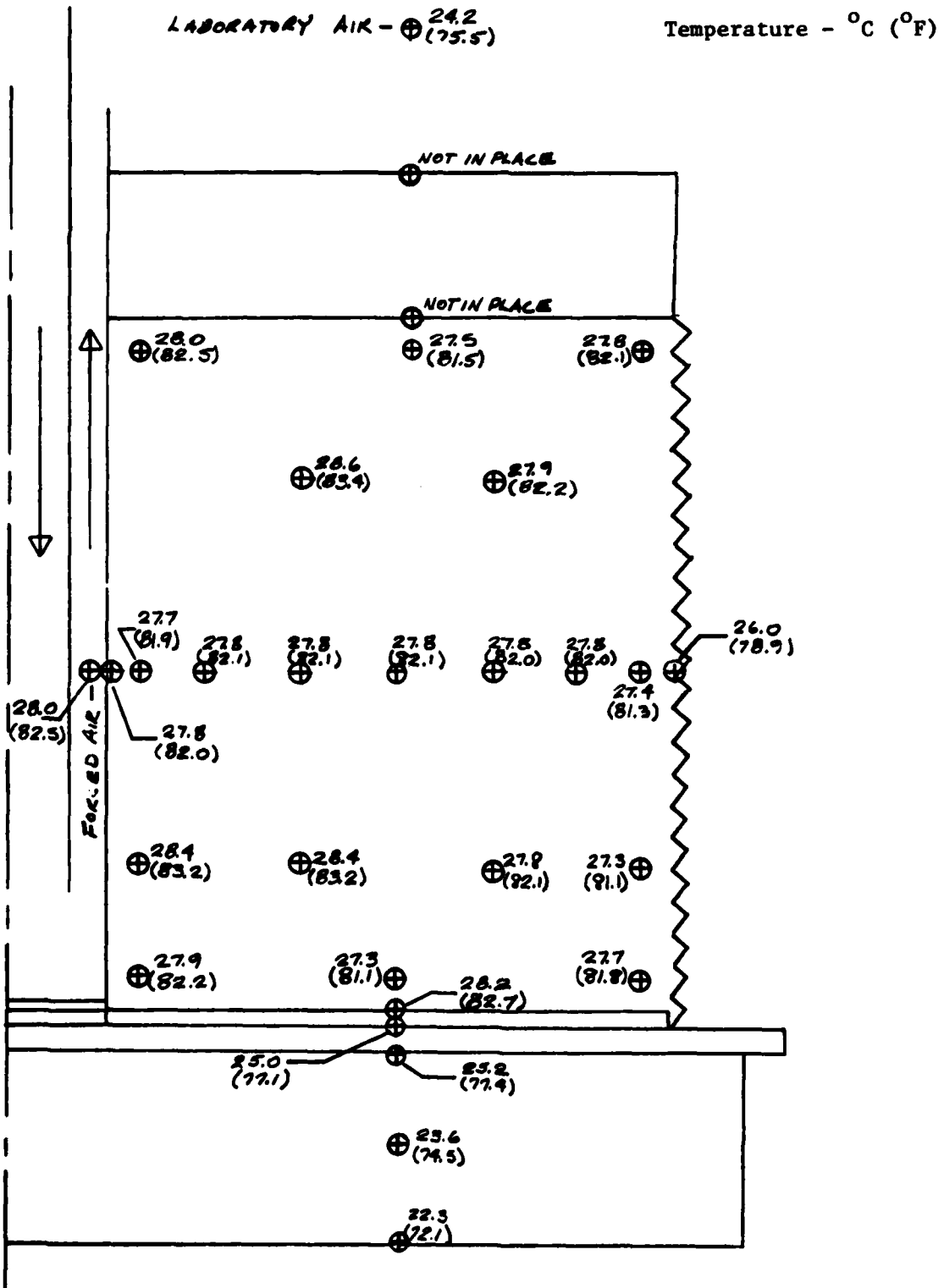


Figure 4a - Axisymmetric temperature distribution measured in HEMSS 3T at end of grout placement (0 hr).

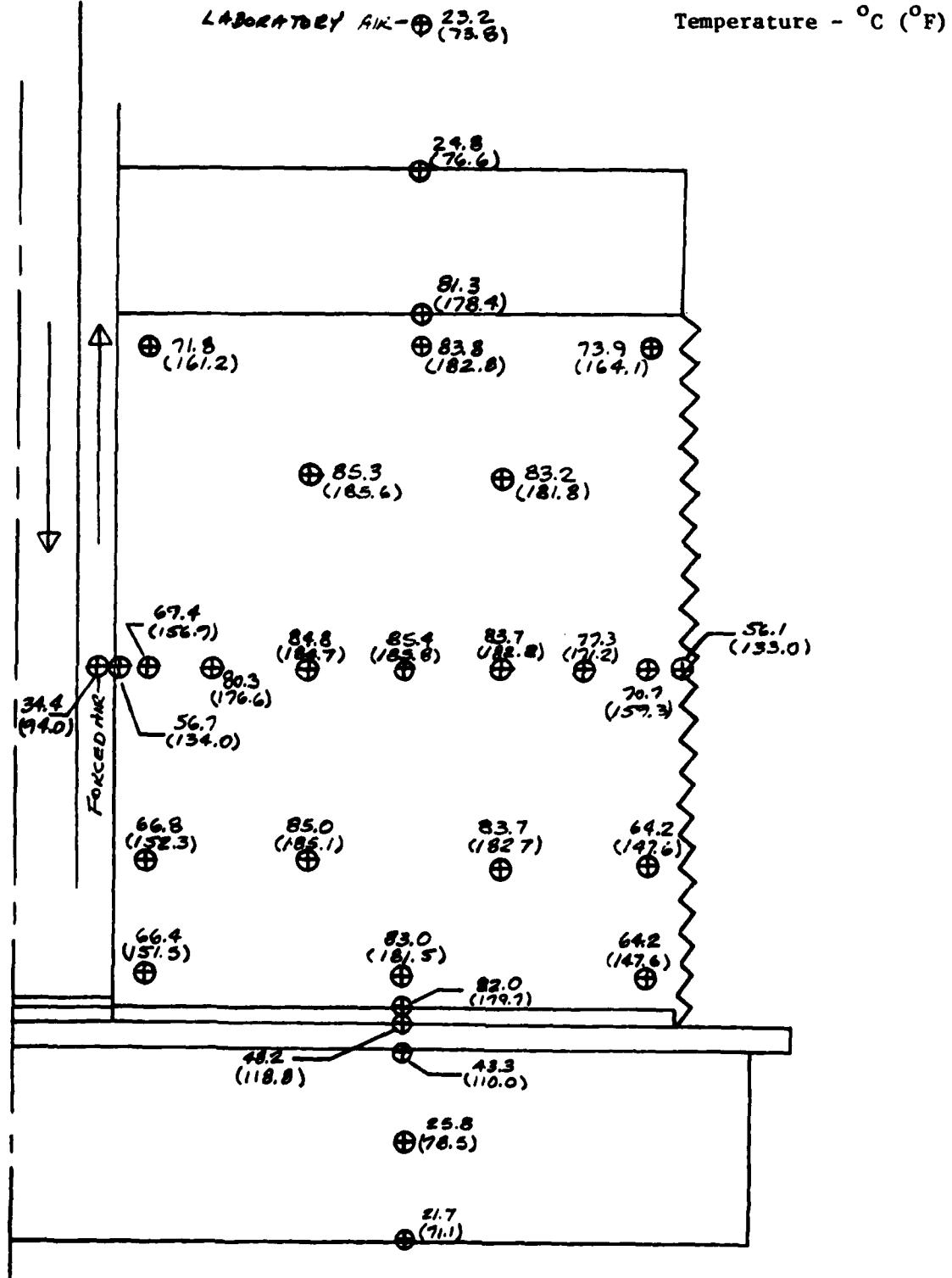


Figure 4b - Axisymmetric temperature distribution measured in HEMSS 3T at 12 hr (0.5 days) after grout placement.

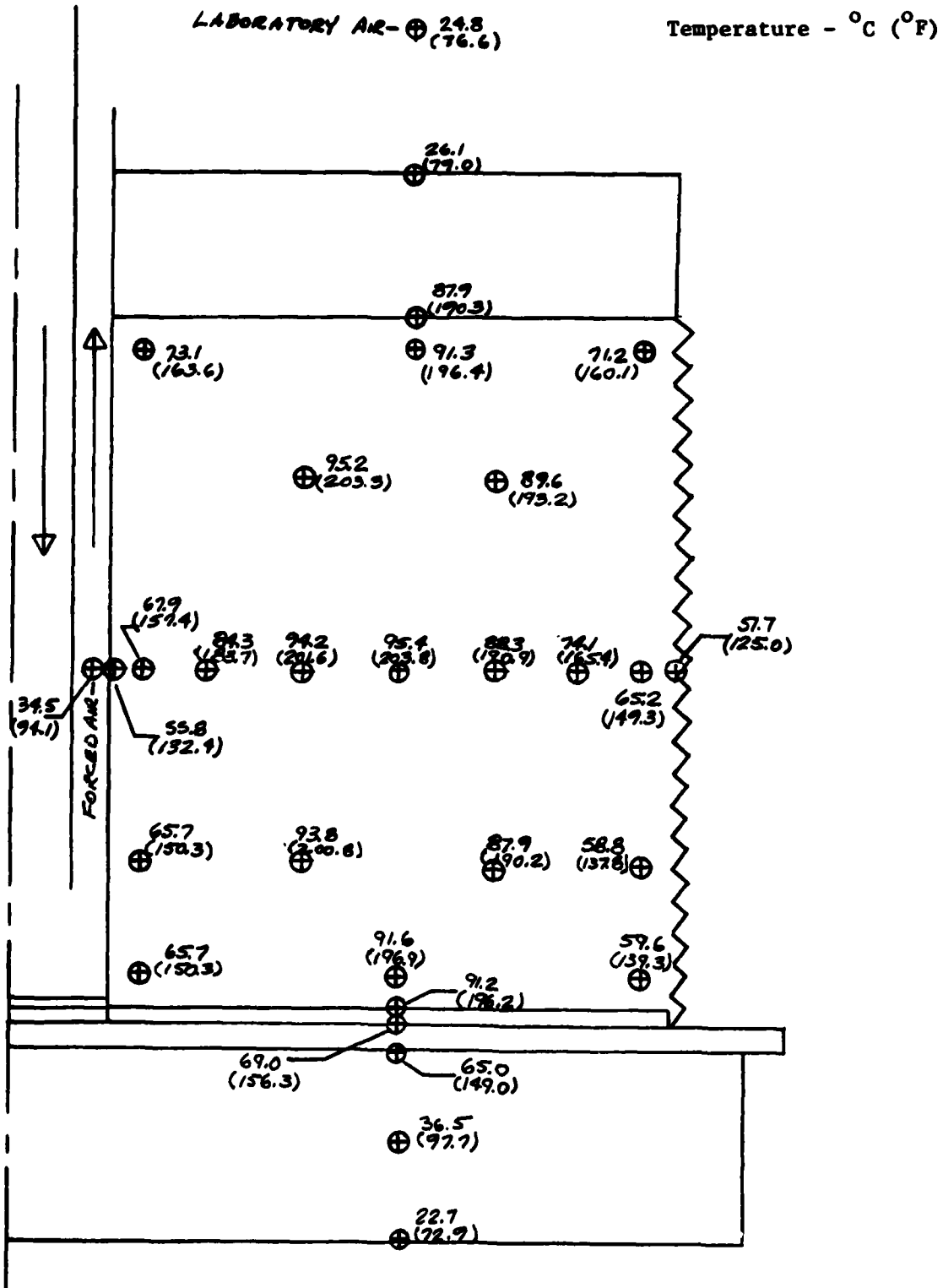


Figure 4c - Axisymmetric temperature distribution measured in HEMSS 3T at 24 hr (1.0 days) after grout placement).

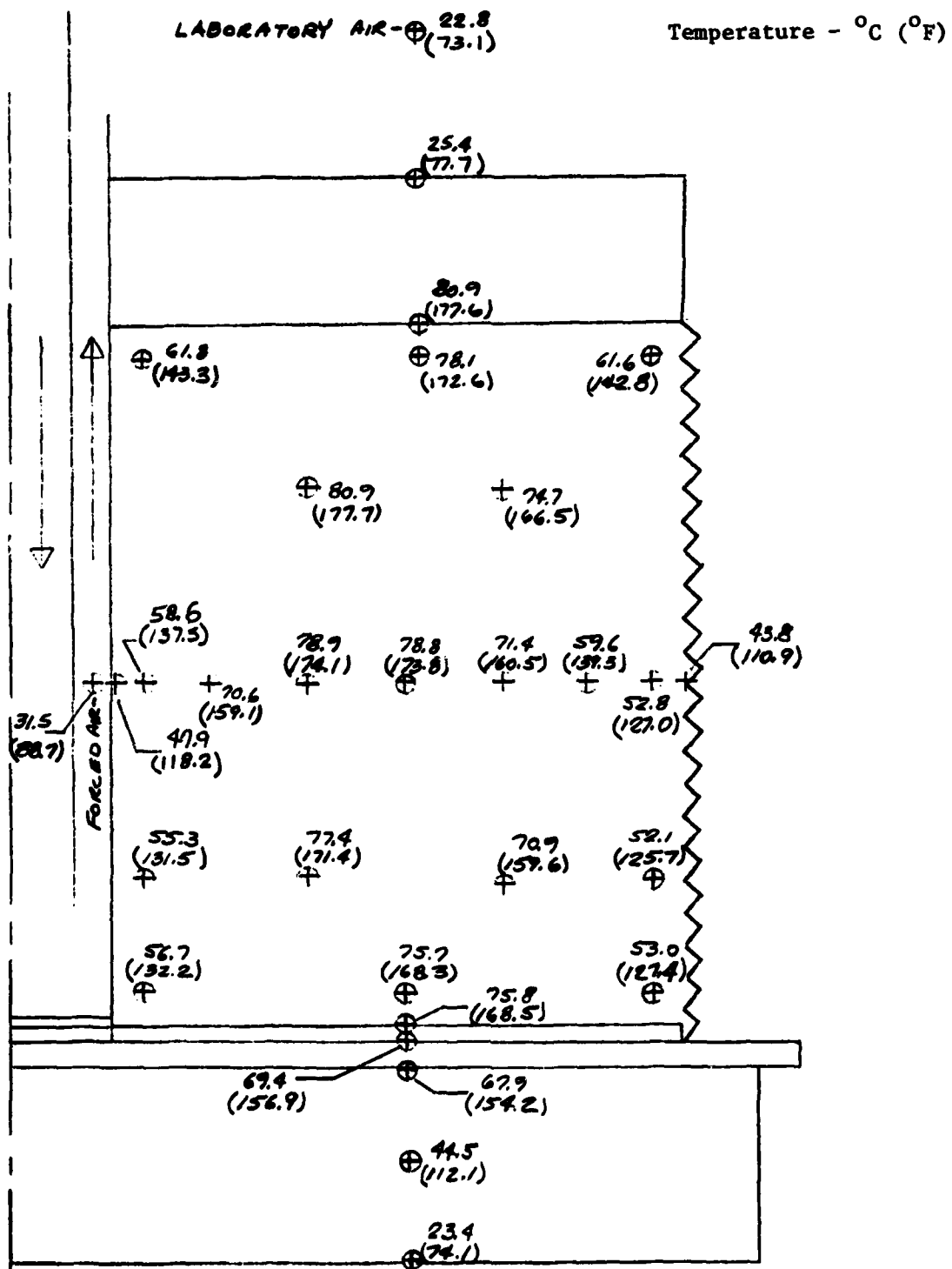


Figure 4d - Axisymmetric temperature distribution measured in HEMSS 3T at 3 days 2 hr (3.08 days) after grout placement.

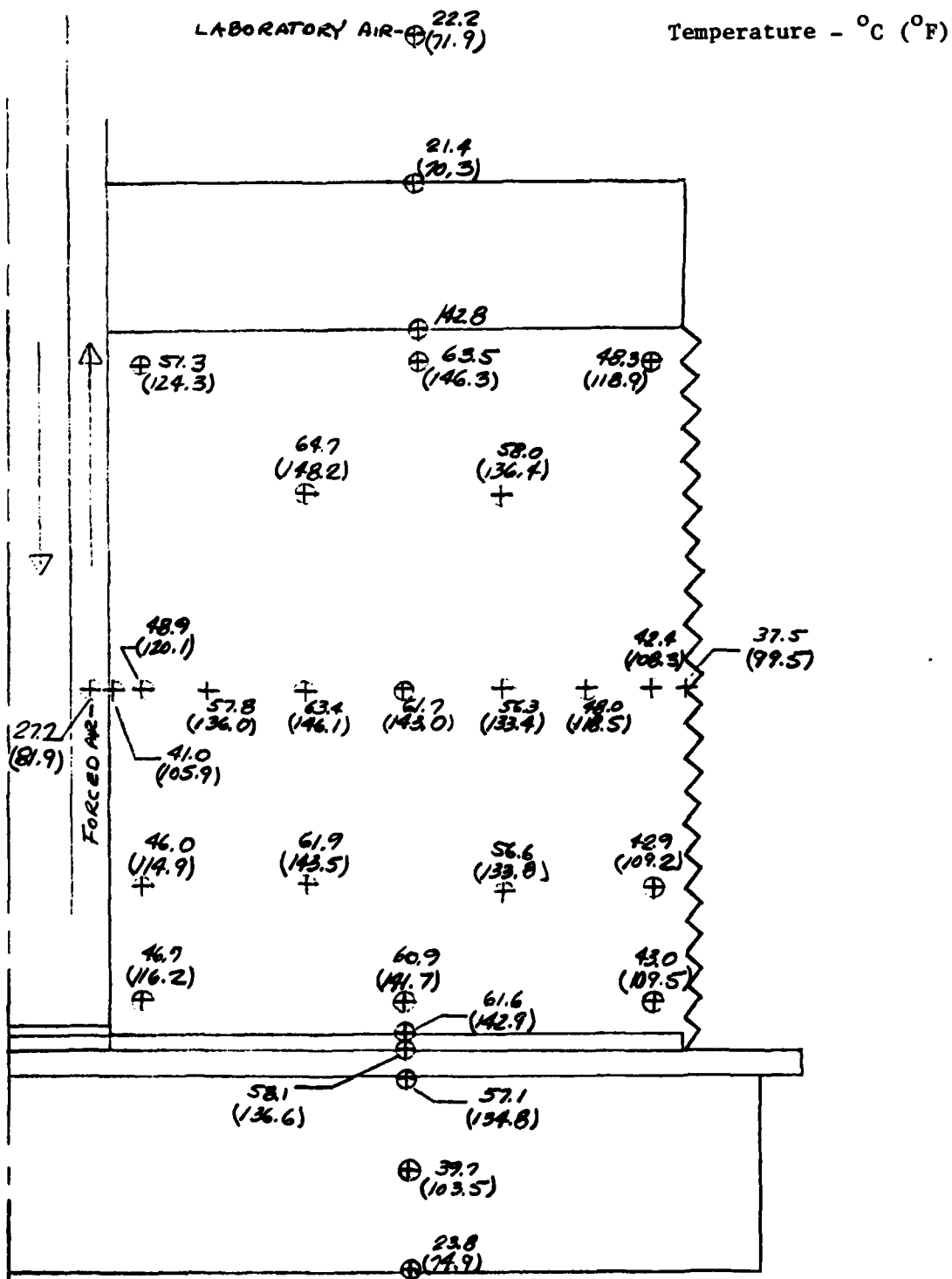


Figure 4e - Axisymmetric temperature distribution measured in HEMSS 3T at 4 days 22 hr (4.92 days) after grout placement.

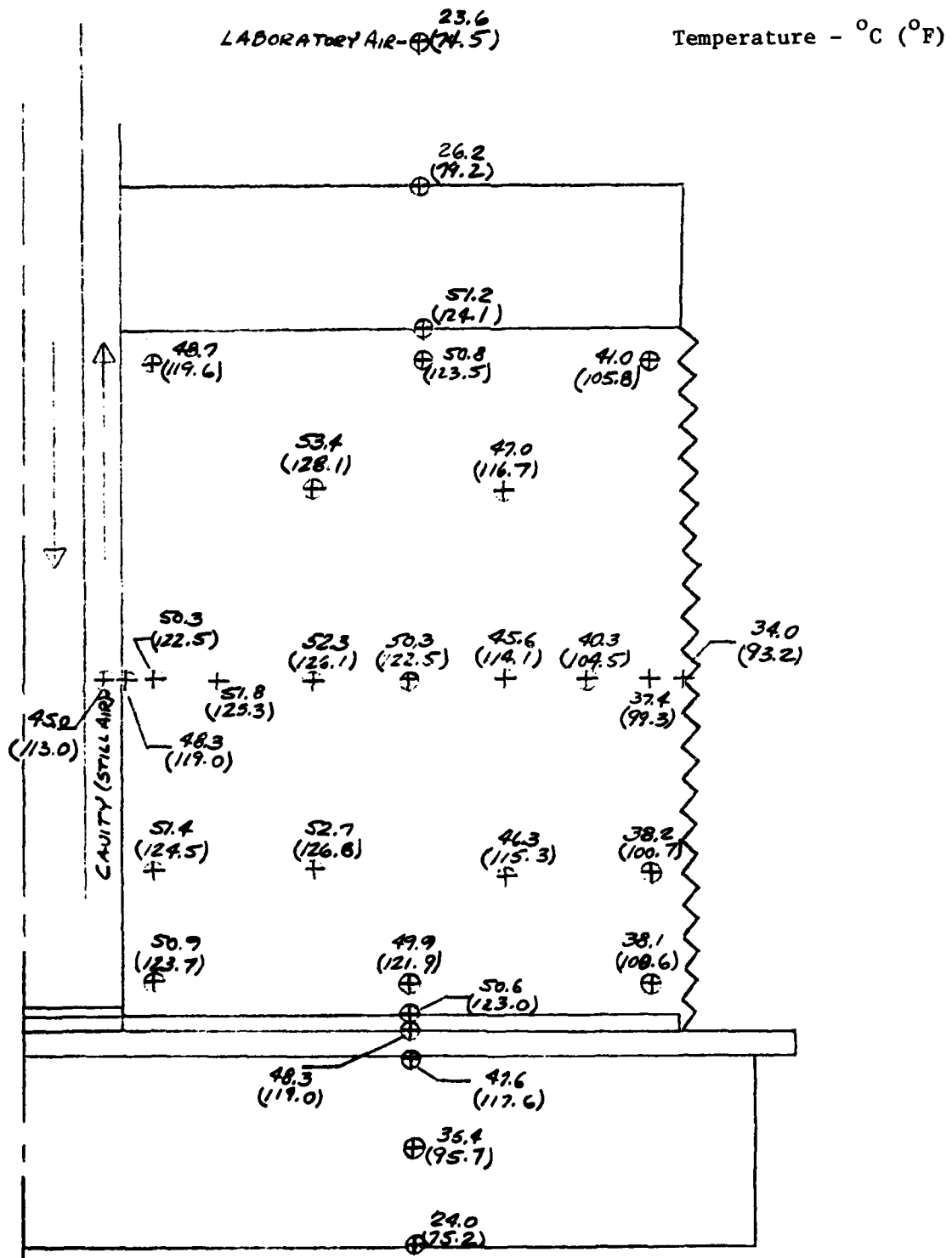


Figure 4f - Axisymmetric temperature distribution measured in HEMSS 3T at 7 days 2 hr (7.08 days) after grout placement.

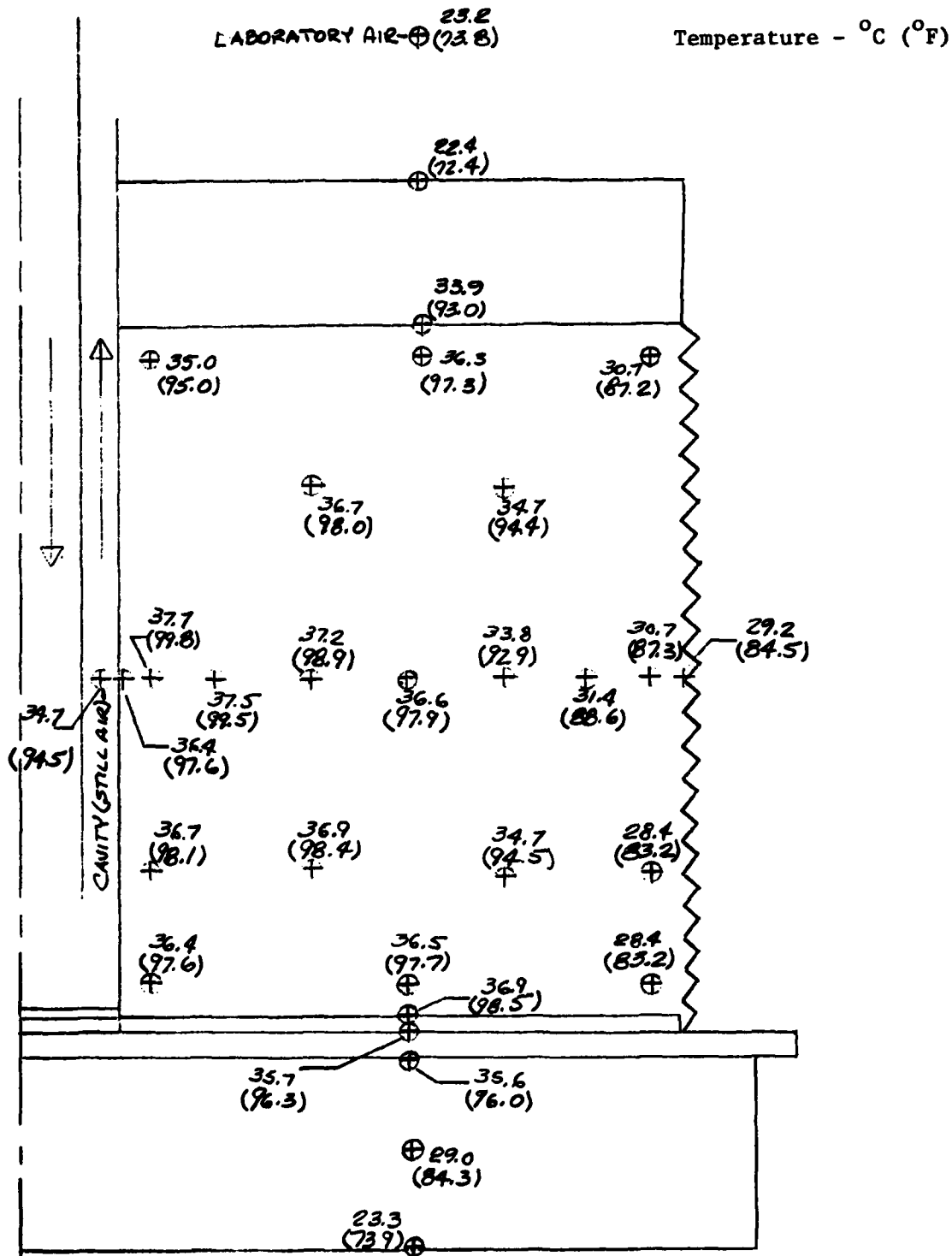


Figure 4g - Axisymmetric temperature distribution measured in HEMSS 3T at 12 days after grout placement.

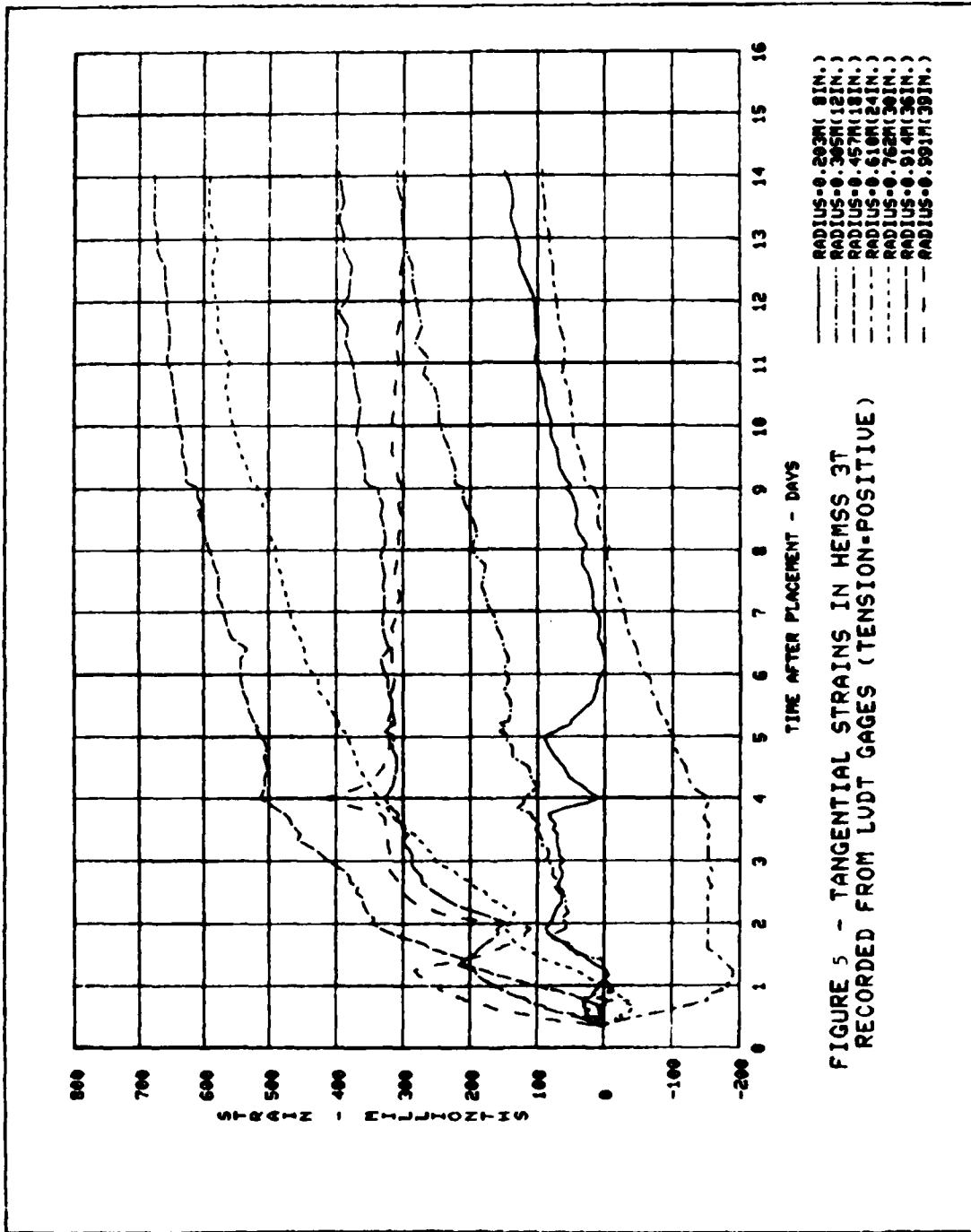


FIGURE 5 - TANGENTIAL STRAINS IN HEMSS 3T
RECORDED FROM LUDT GAGES (TENSION-POSITIVE)

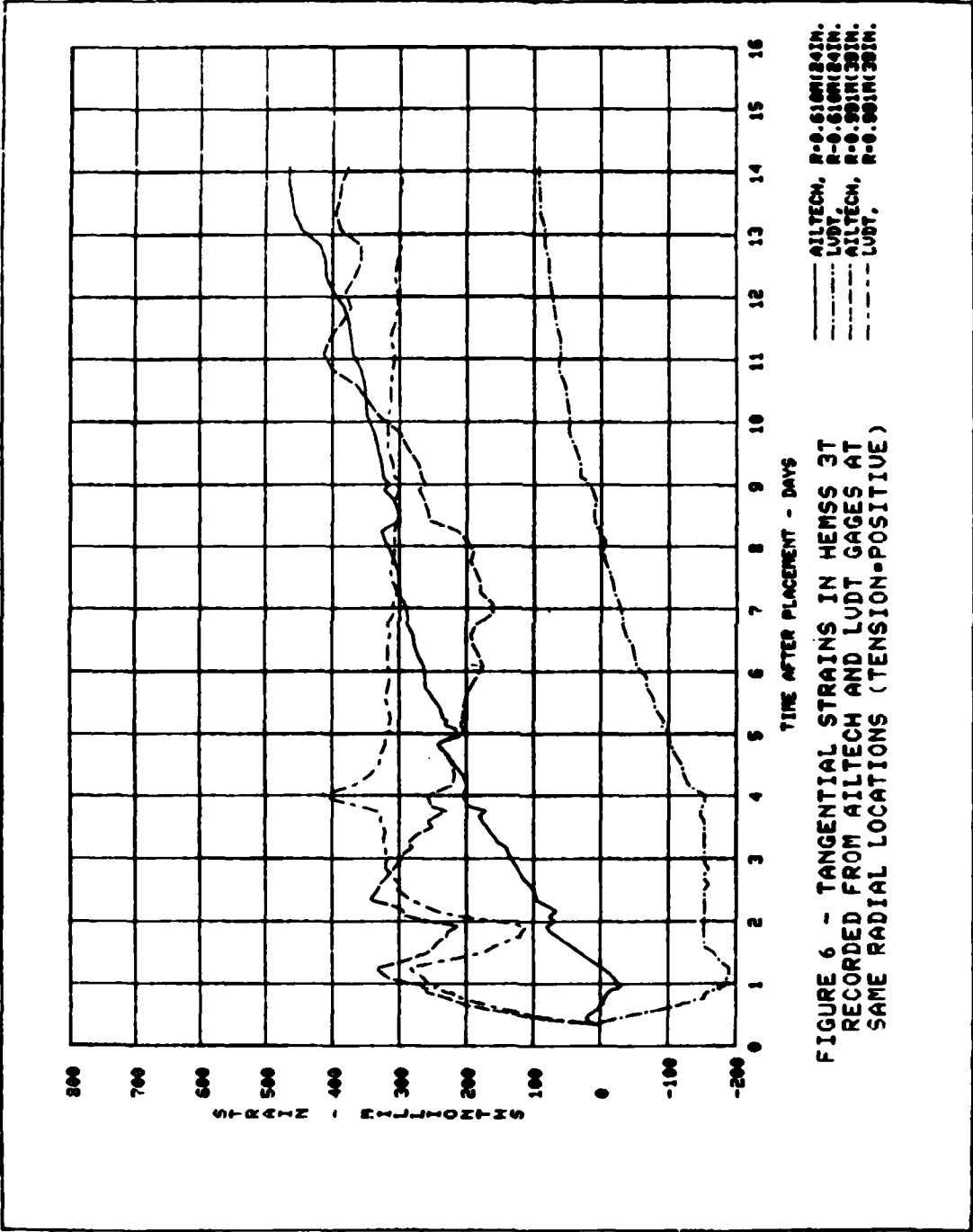
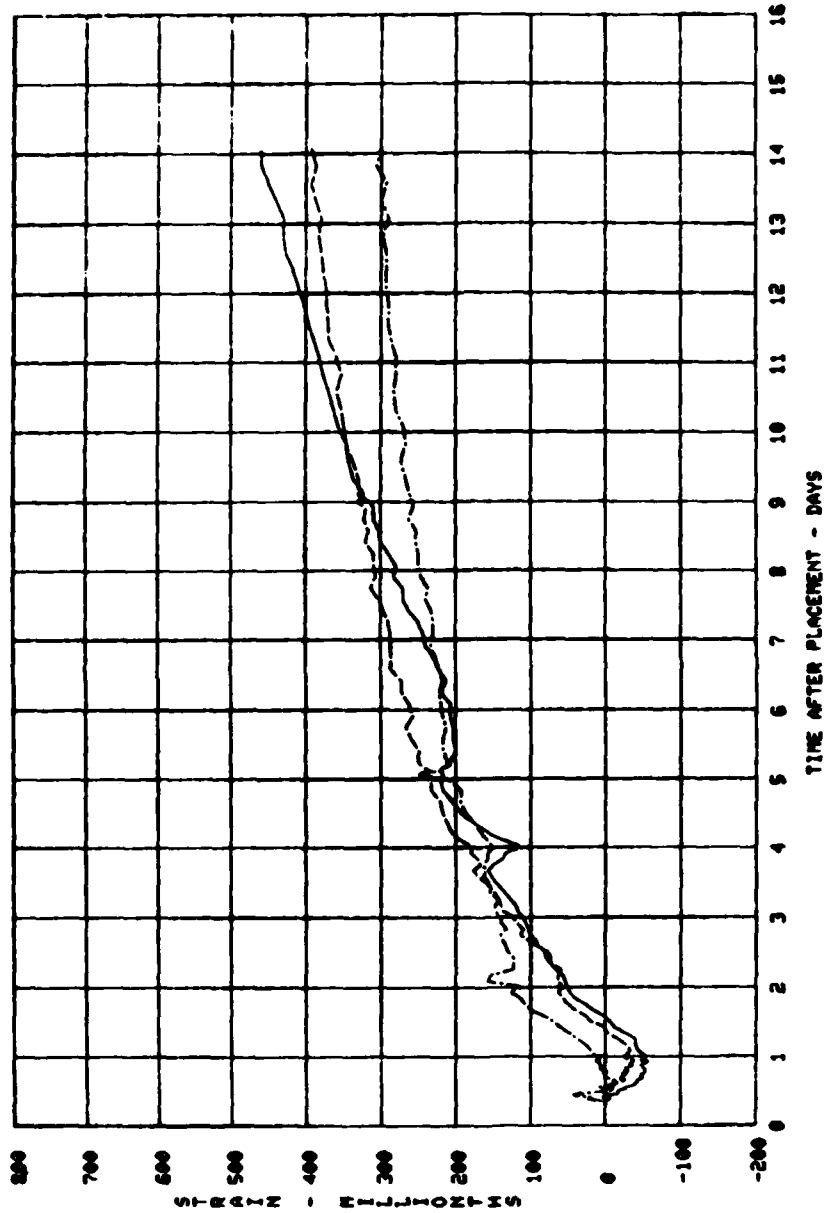


FIGURE 6 - TANGENTIAL STRAINS IN HEMSS 3T
 RECORDED FROM AILTECH AND LVDI GAGES AT
 SAME RADIAL LOCATIONS (TENSION=POSITIVE)



--- RADIUS=0.305R(12IN.)
 - - - RADIUS=0.610R(24IN.)
 - · - RADIUS=0.914R(36IN.)

FIGURE 7 - RADIAL STRAINS IN HEMSS 3T RECORDED FROM LUDT GAGES (TENSION=POSITIVE)

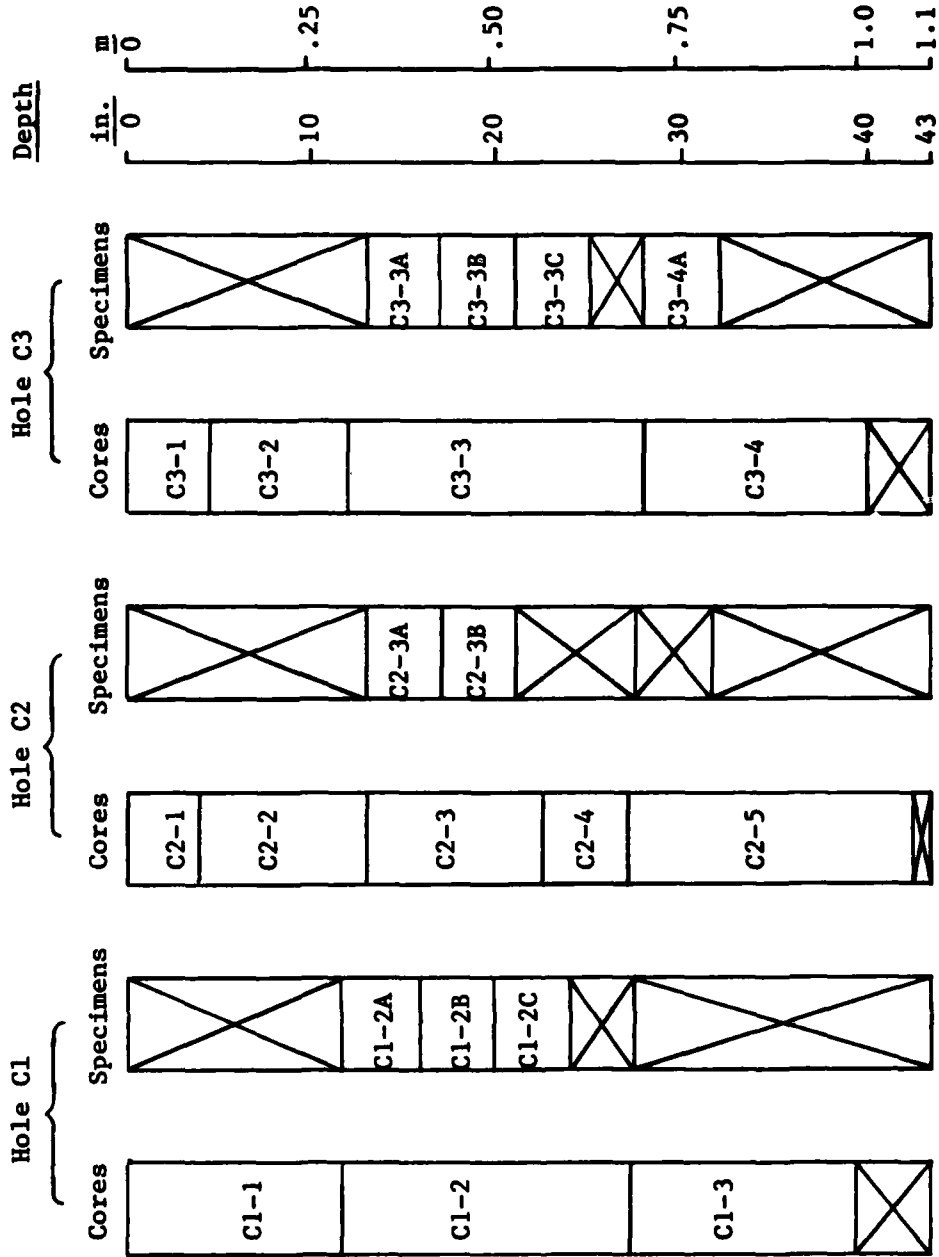


Figure 8a - Core logs and specimen locations for 7-day, C-series tests of 2C4 grout from HEMSS 3T at radius = 0.61 m (24 in.).

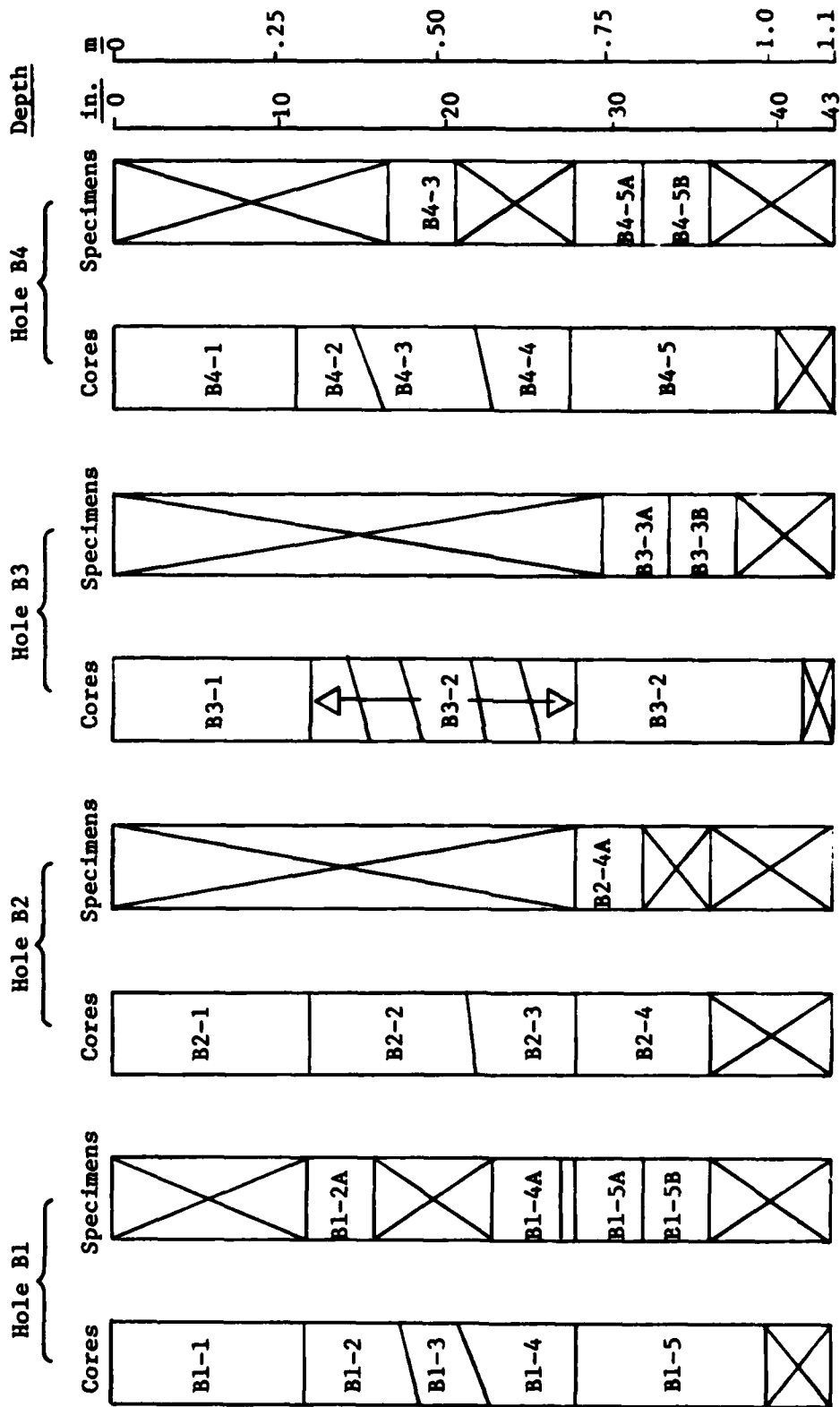


Figure 8b - Core logs and specimen locations for 7-day, B-series tests of 2C4 grout from HEMSS 3T at radius = 0.91 m (36 in.).

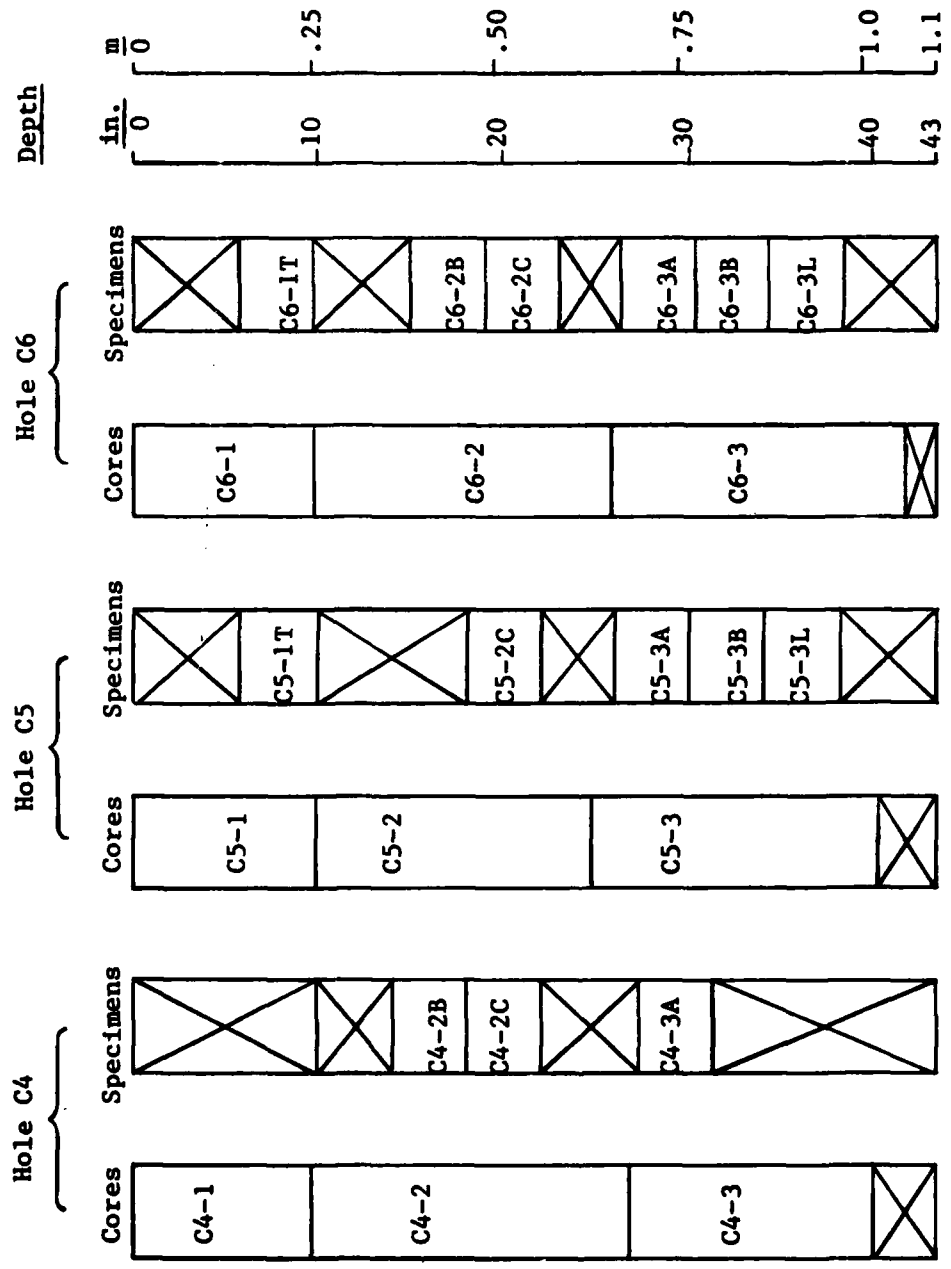


Figure 8c - Core logs and specimen locations for 14-day, C-series tests of 2C4 grout from HEMSS 3T at radius = 0.61 m (24 in.).

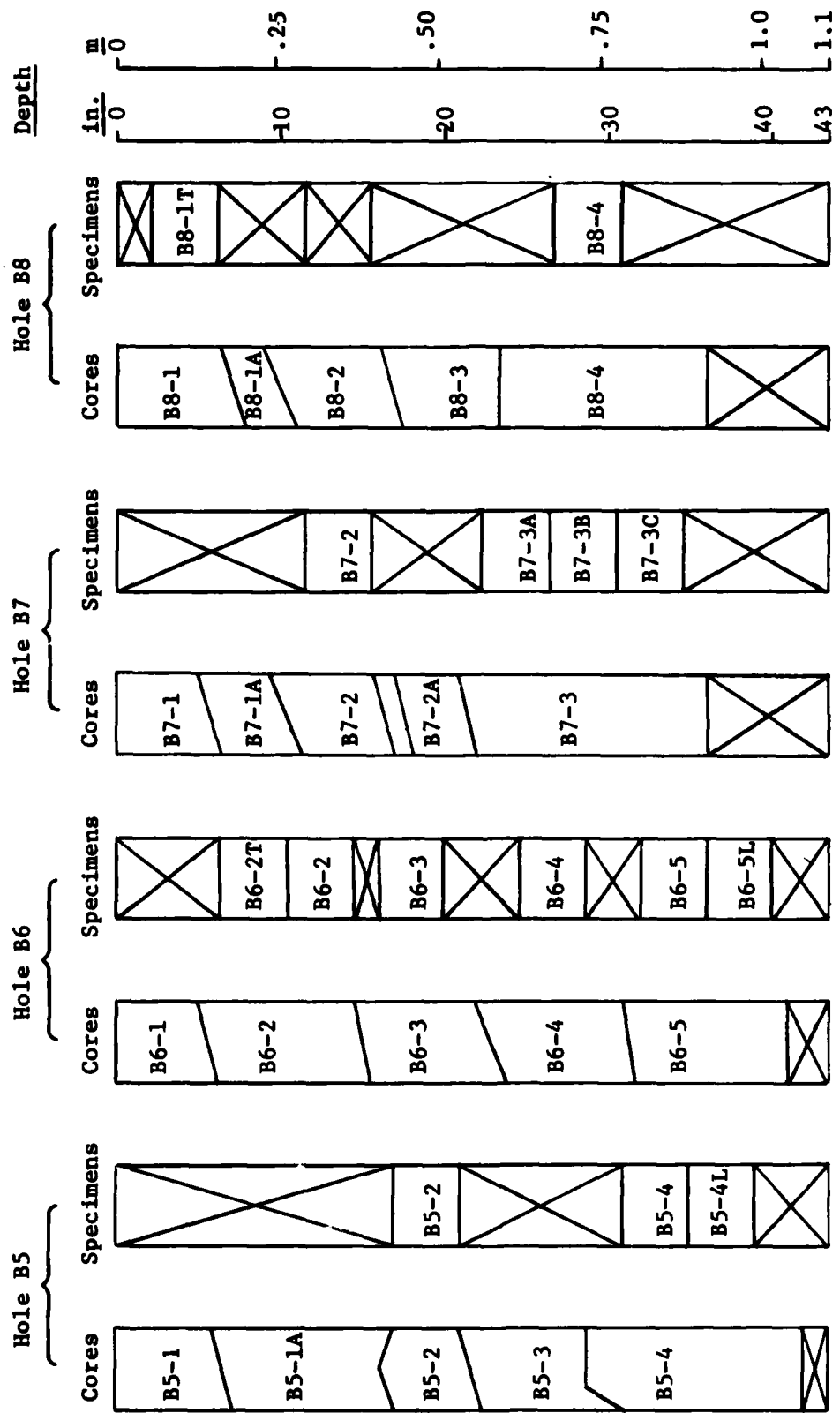


Figure 8d - Core logs and specimen locations for 14-day, B-series test of 2C4 grout from HEMSS 3T at radius = 0.91 m (36 in.).

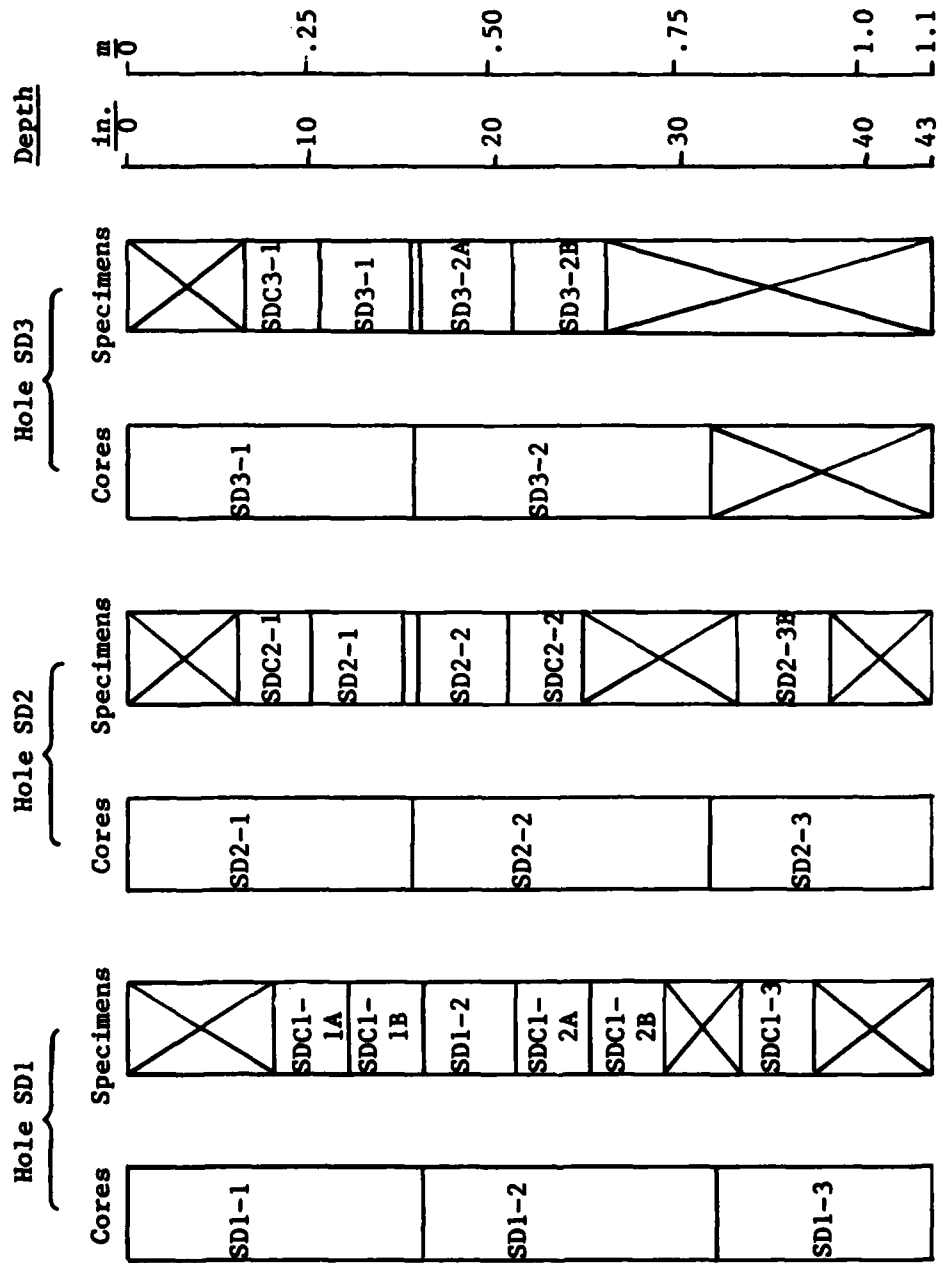


Figure 8e - Core logs and specimen locations for 14-day, SD-series tests of 2C4 grout from HEMSS 3T at radius = 0.61 m (24 in.).

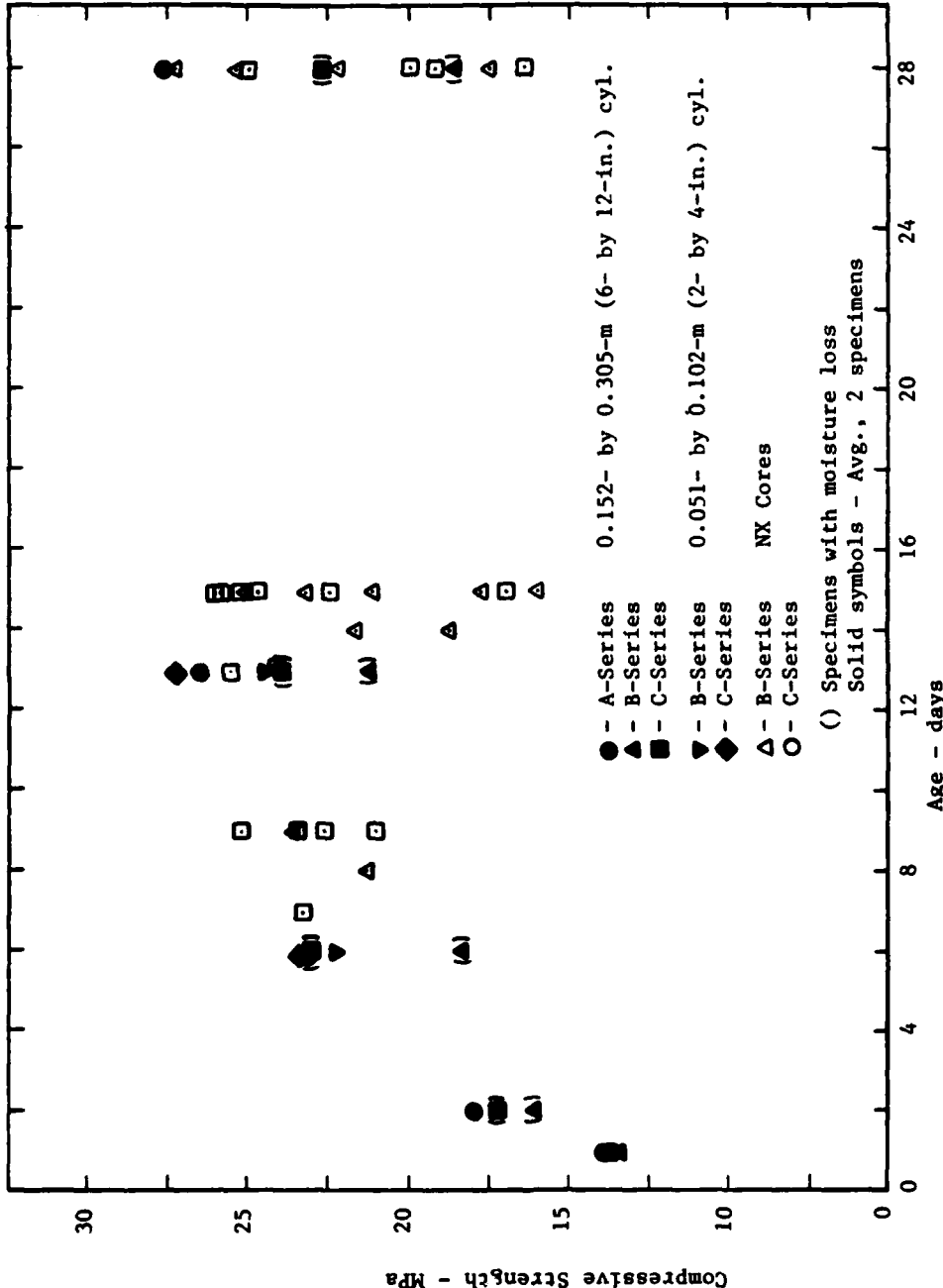


Figure 9. Summary of results of all unconfined compressive strength tests conducted on cast and cored 2C4 grout specimens.

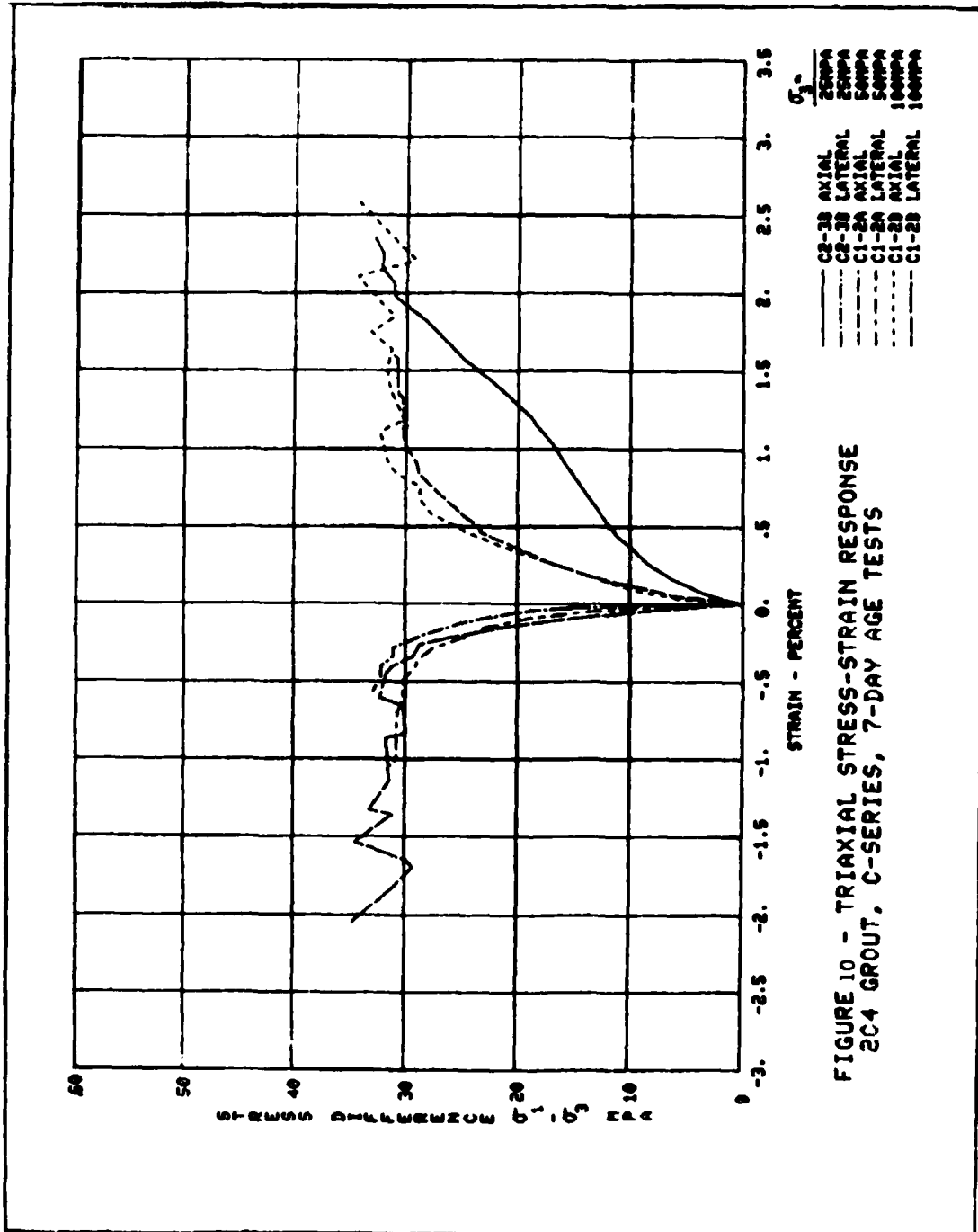
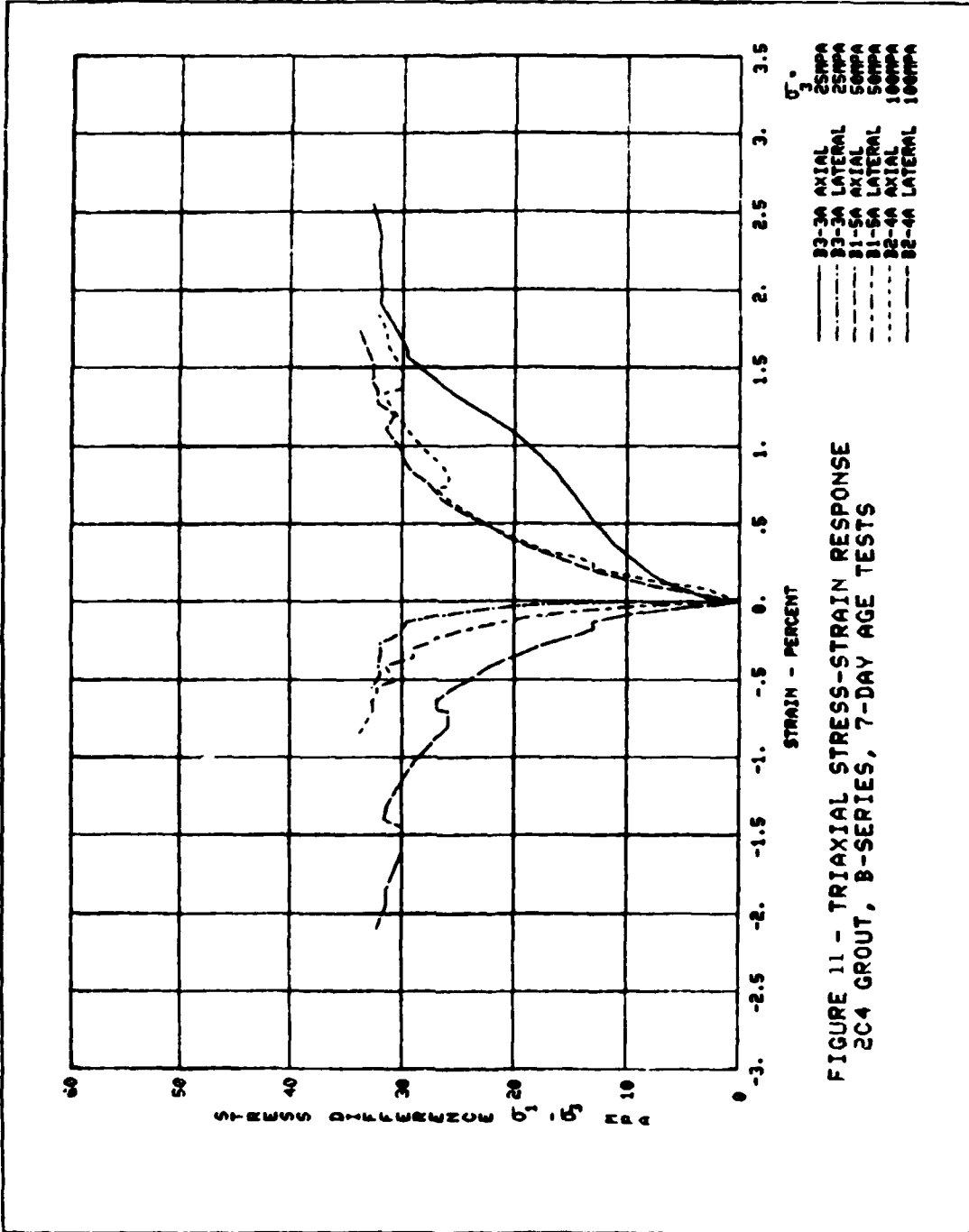


FIGURE 10 - TRIAXIAL STRESS-STRAIN RESPONSE
204 GROUT, C-SERIES, 7-DAY AGE TESTS



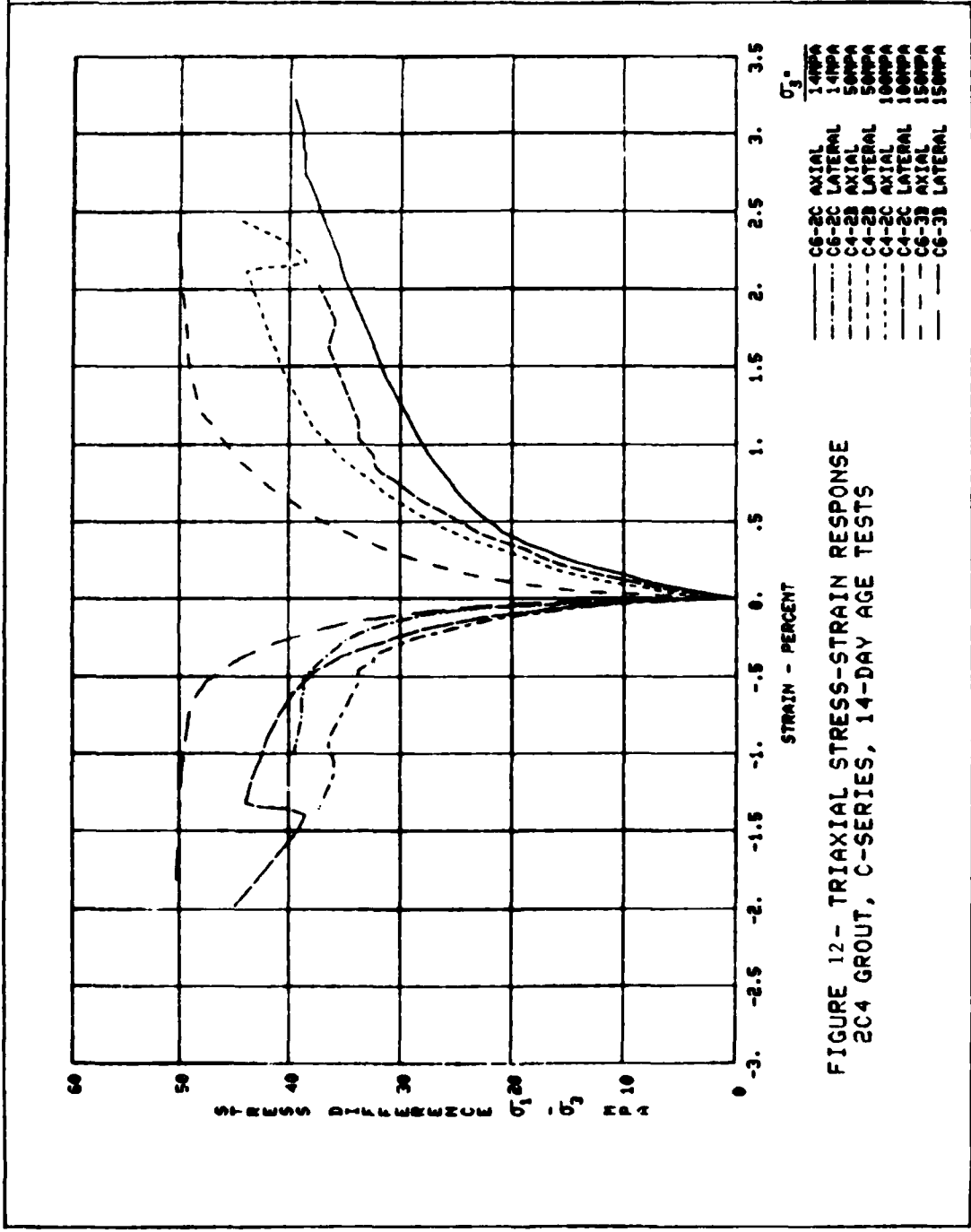
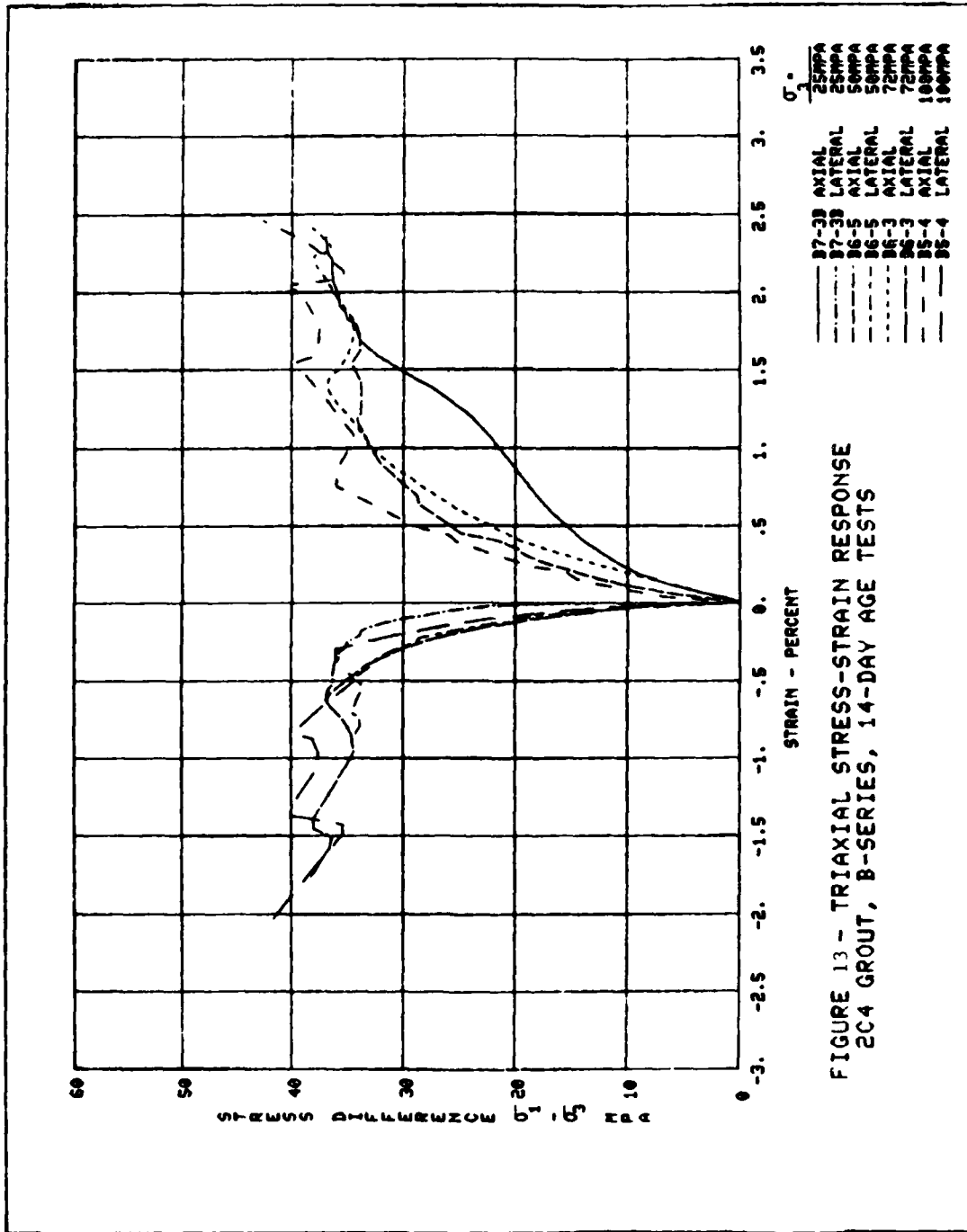


FIGURE 12- TRIAXIAL STRESS-STRAIN RESPONSE
2C4 GROUT, C-SERIES, 14-DAY AGE TESTS



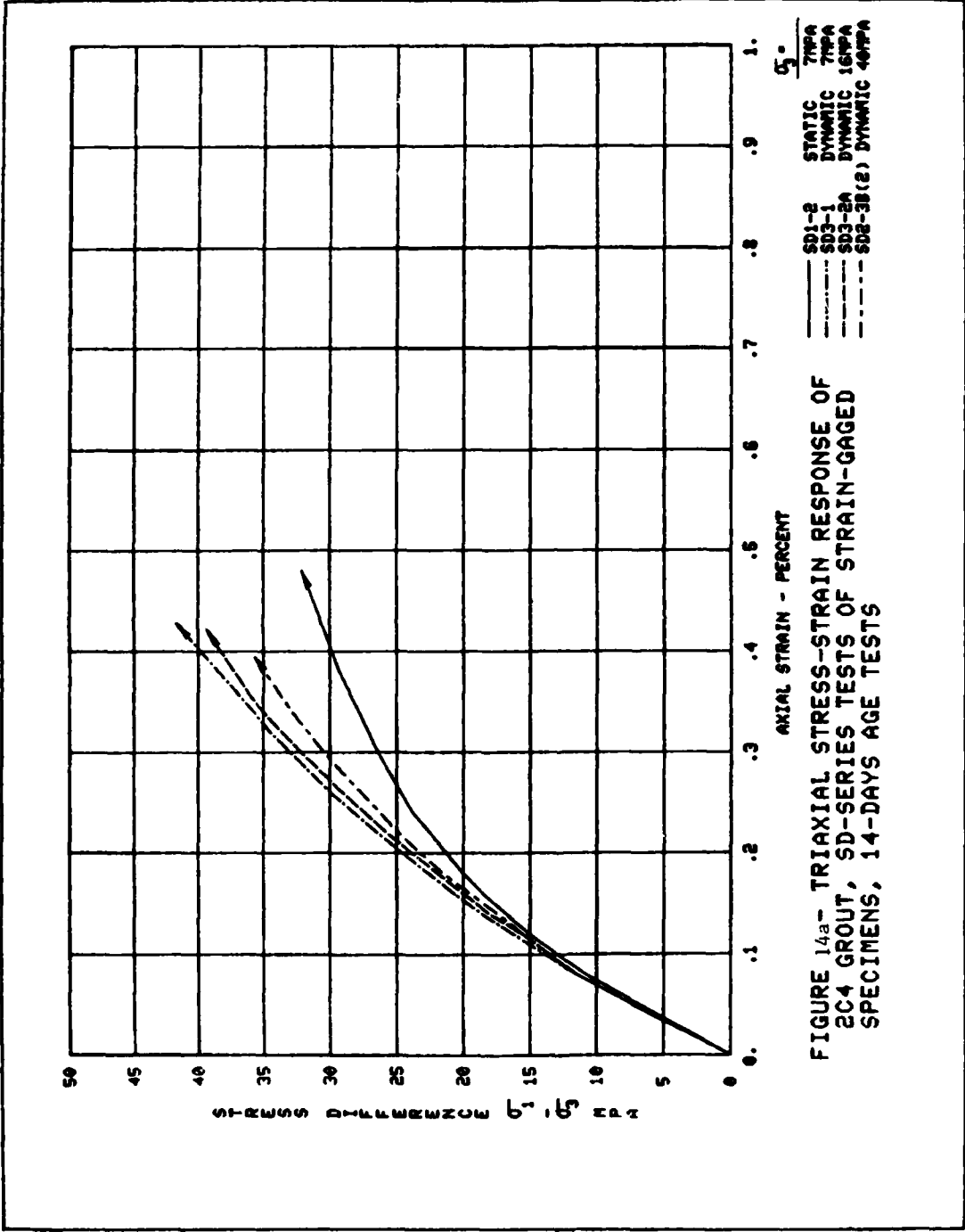


FIGURE 14a- TRIAXIAL STRESS-STRAIN RESPONSE OF 204 GROUT, SD-SERIES TESTS OF STRAIN-GAGED SPECIMENS, 14-DAYS AGE TESTS

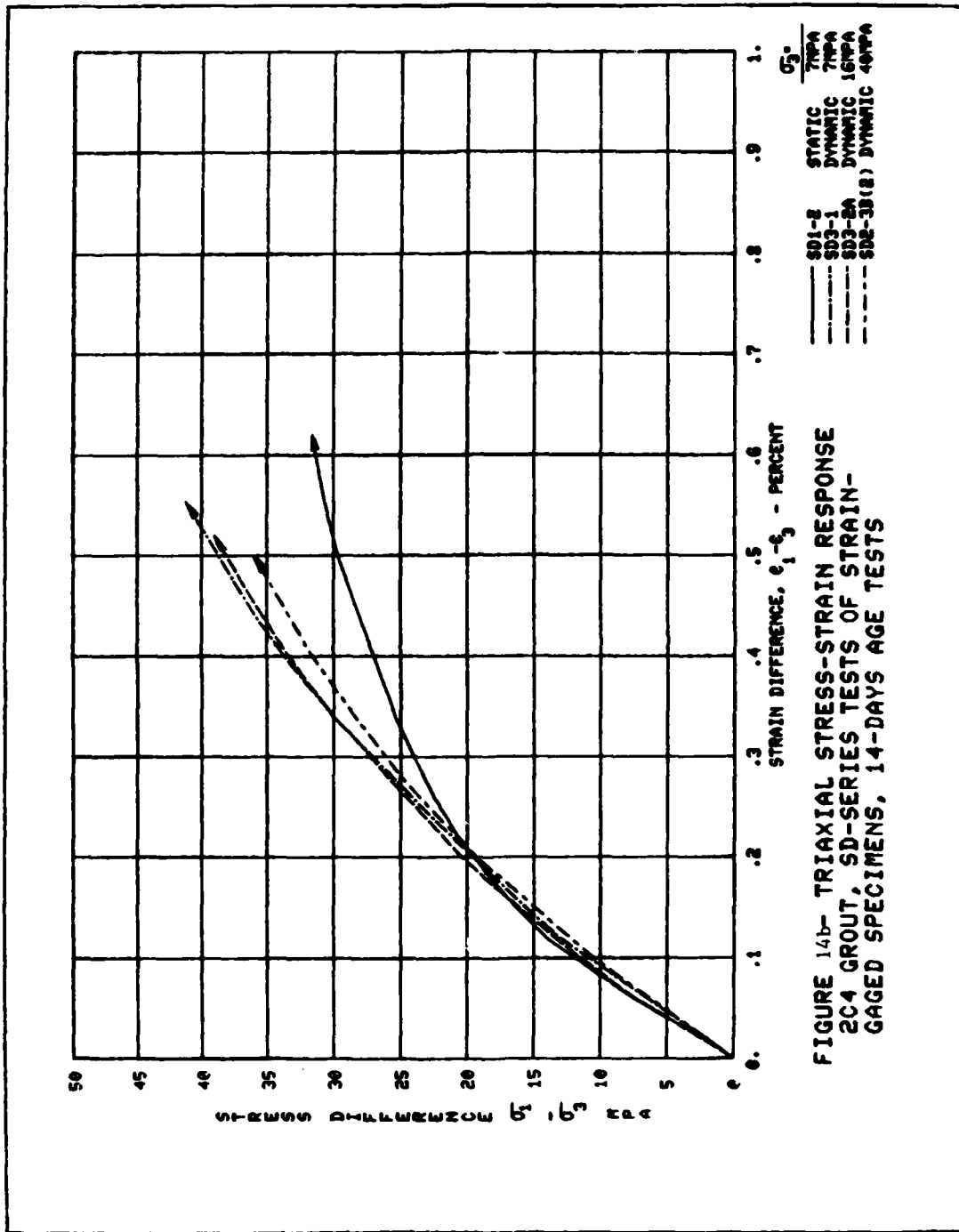


FIGURE 14b- TRIAXIAL STRESS-STRAIN RESPONSE
 2C4 GROUT, SD-SERIES TESTS OF STRAIN-
 GAGED SPECIMENS, 14-DAYS AGE TESTS

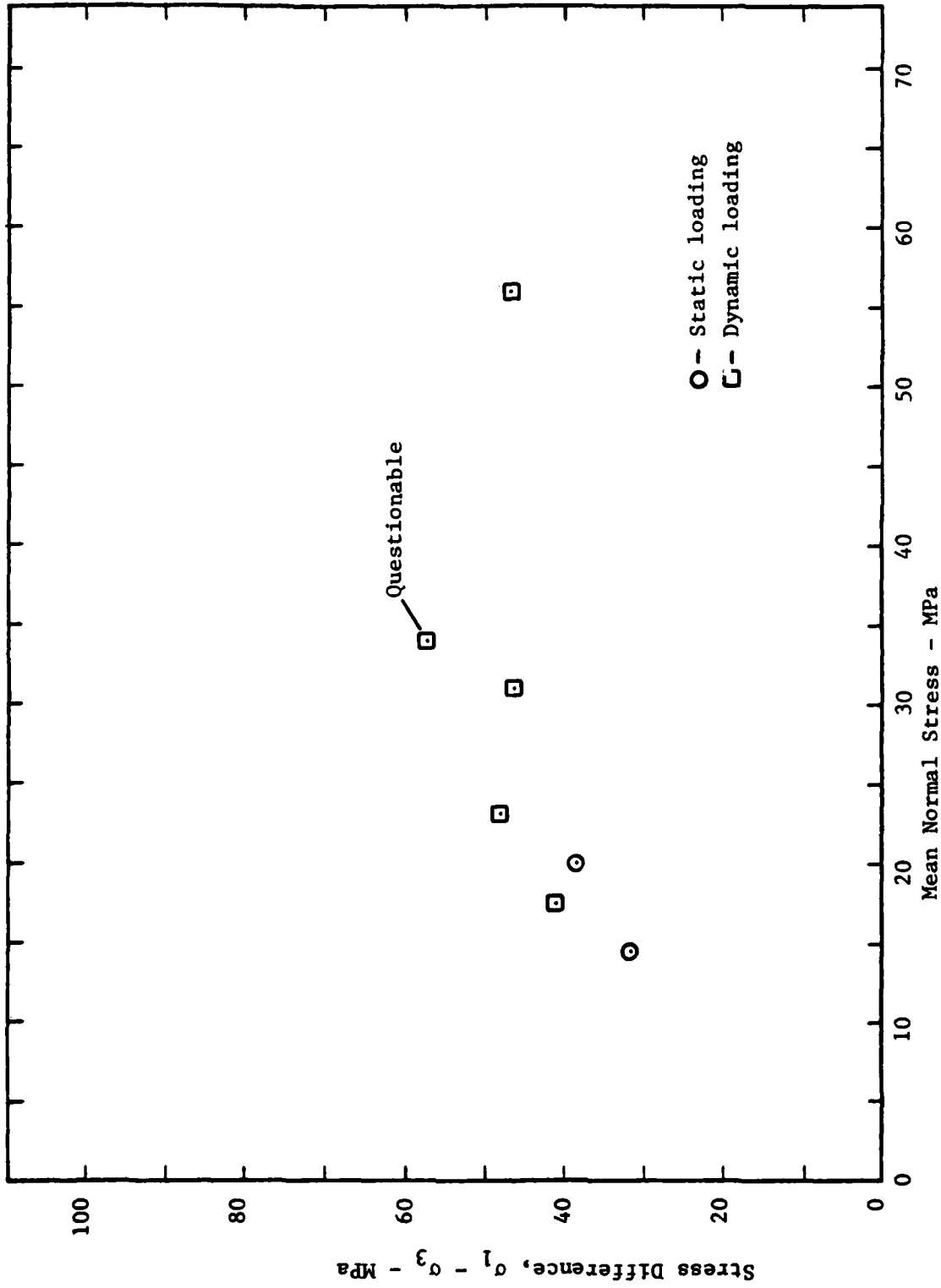
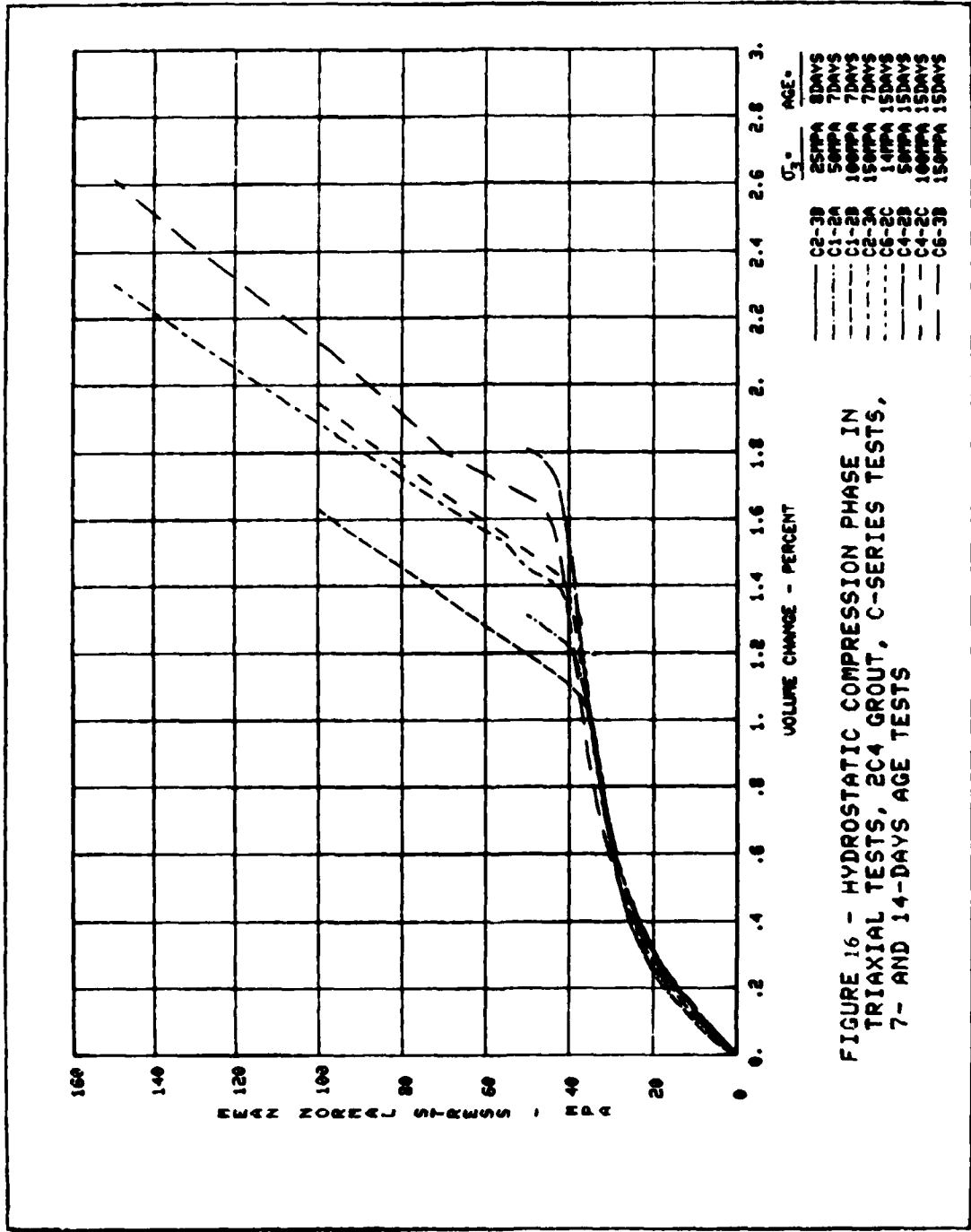


Figure 15. Maximum shear strength of SD-Series, 2C4 grout specimens.



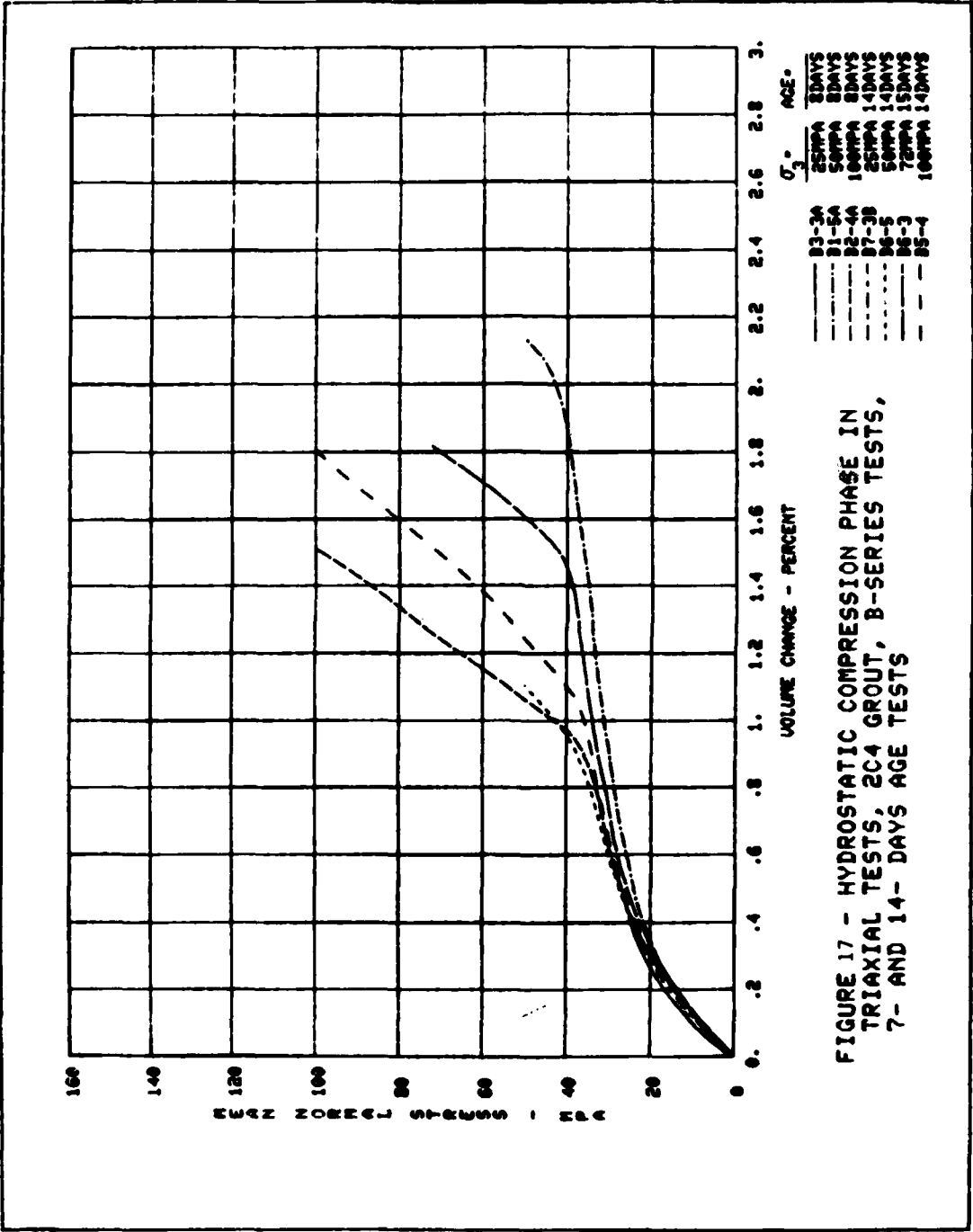
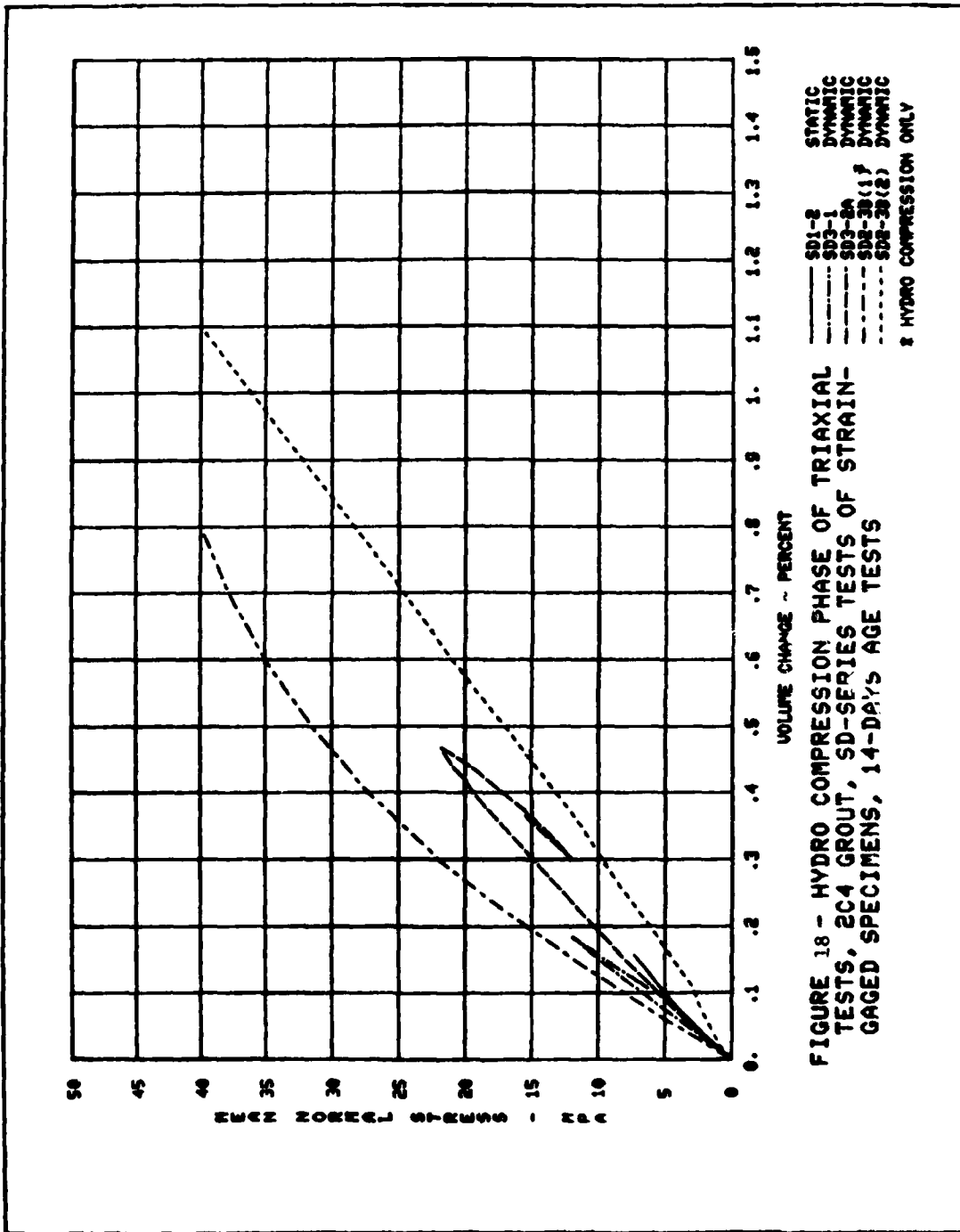


FIGURE 17 - HYDROSTATIC COMPRESSION PHASE IN TRIAXIAL TESTS, 2C4 GROUT, B-SERIES TESTS, 7- AND 14- DAYS AGE TESTS



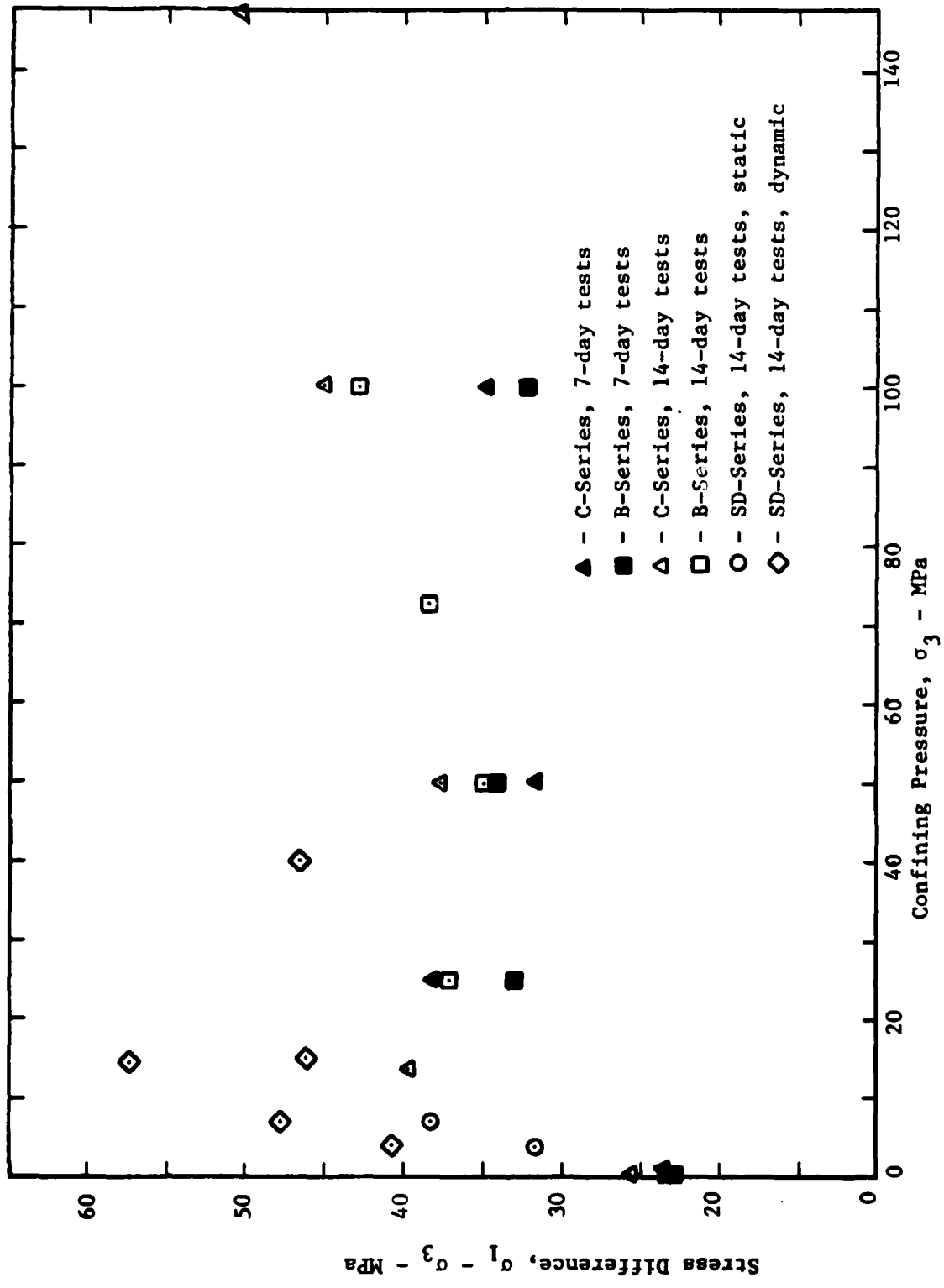


Figure 19. Triaxial compression response of 2C4 grout.

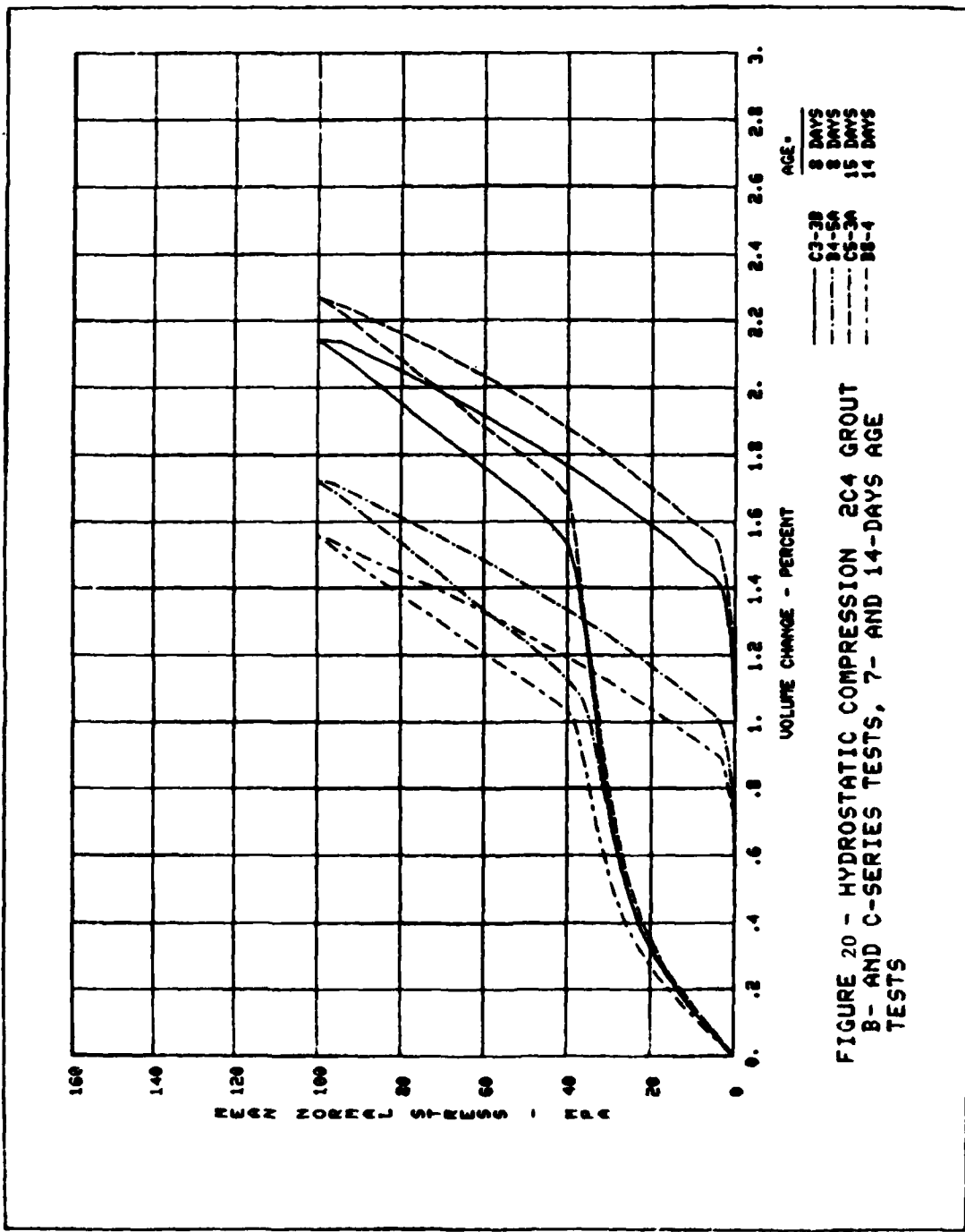


FIGURE 20 - HYDROSTATIC COMPRESSION 20C4 GROUT
B- AND C-SERIES TESTS, 7- AND 14-DAYS AGE
TESTS

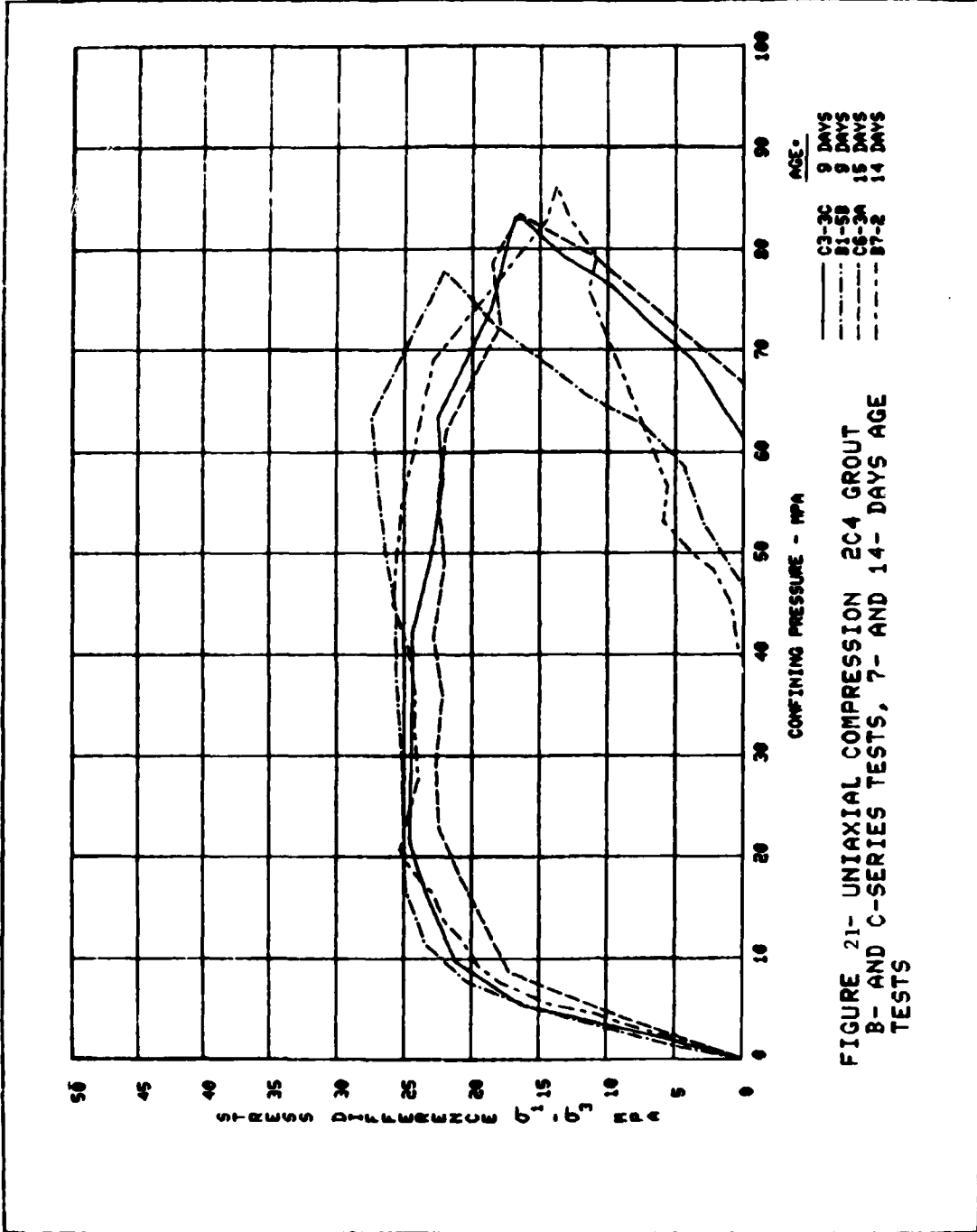
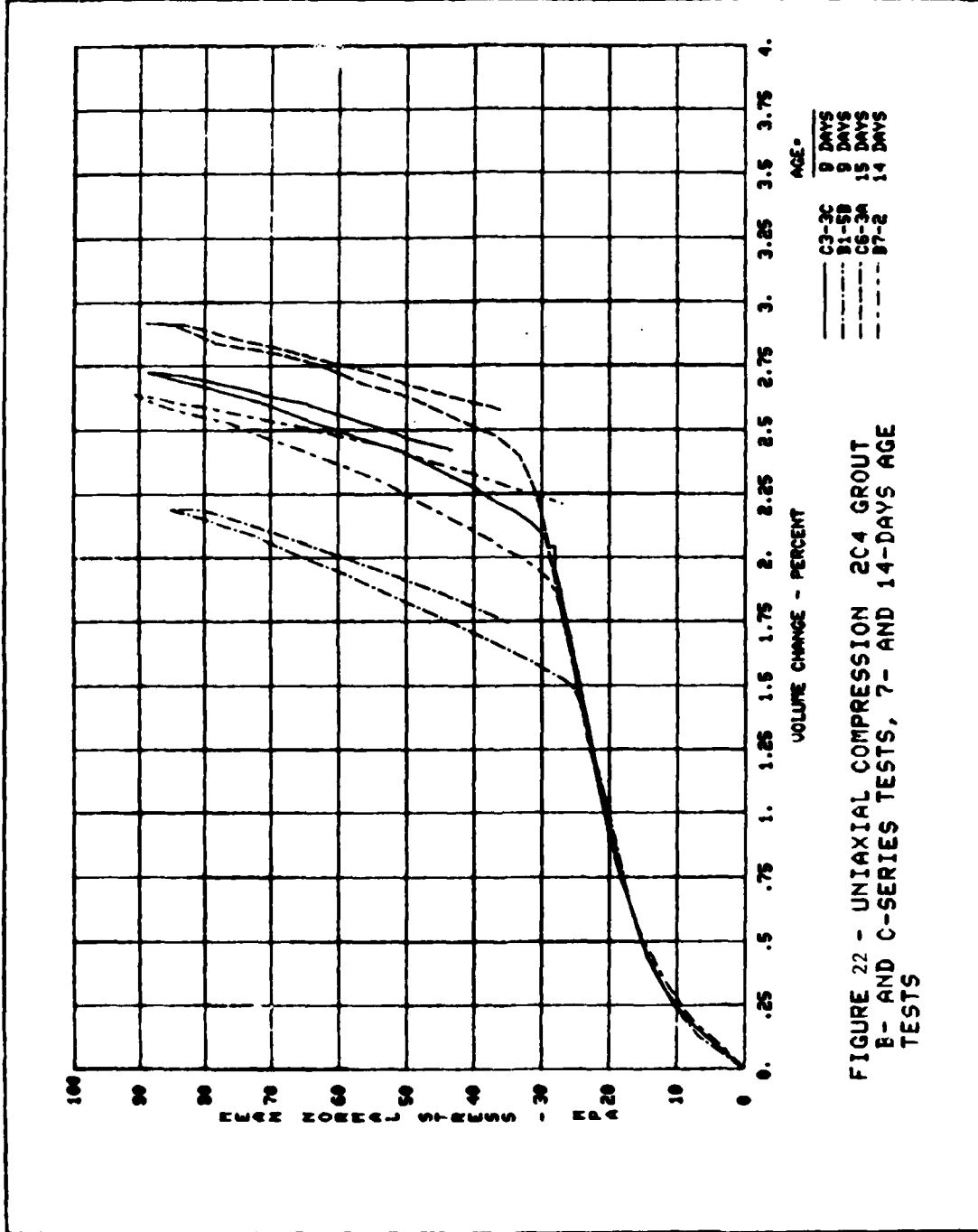


FIGURE 21- UNIAXIAL COMPRESSION 204 GROUT
B- AND C-SERIES TESTS, 7- AND 14- DAYS AGE
TESTS



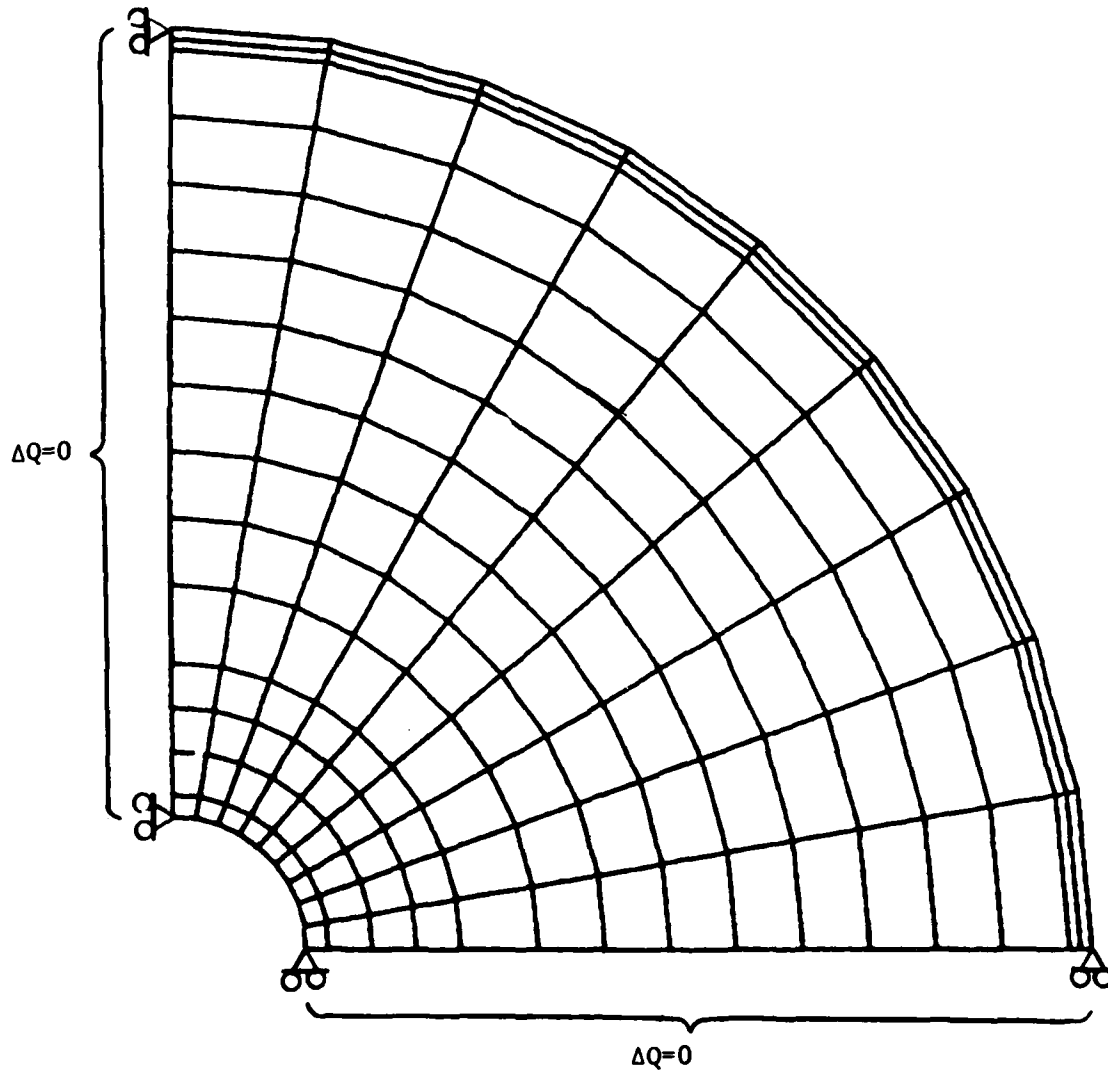


Figure 23 - Finite-element model, quarter section of horizontal plan used in temperature and stress-strain simulations.

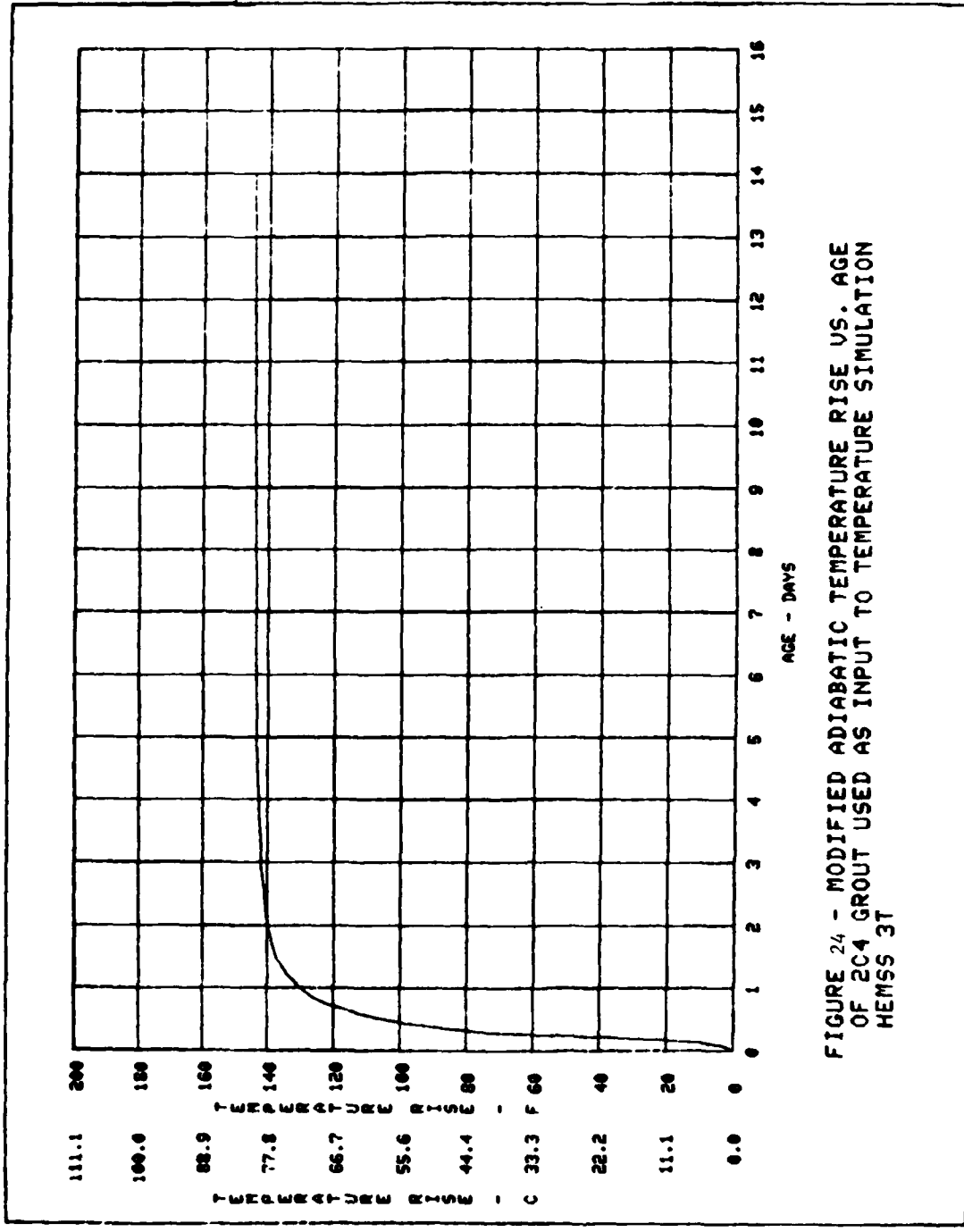


FIGURE 24 - MODIFIED ADIABATIC TEMPERATURE RISE VS. AGE OF 2C4 GROUT USED AS INPUT TO TEMPERATURE SIMULATION HEMSS 3T

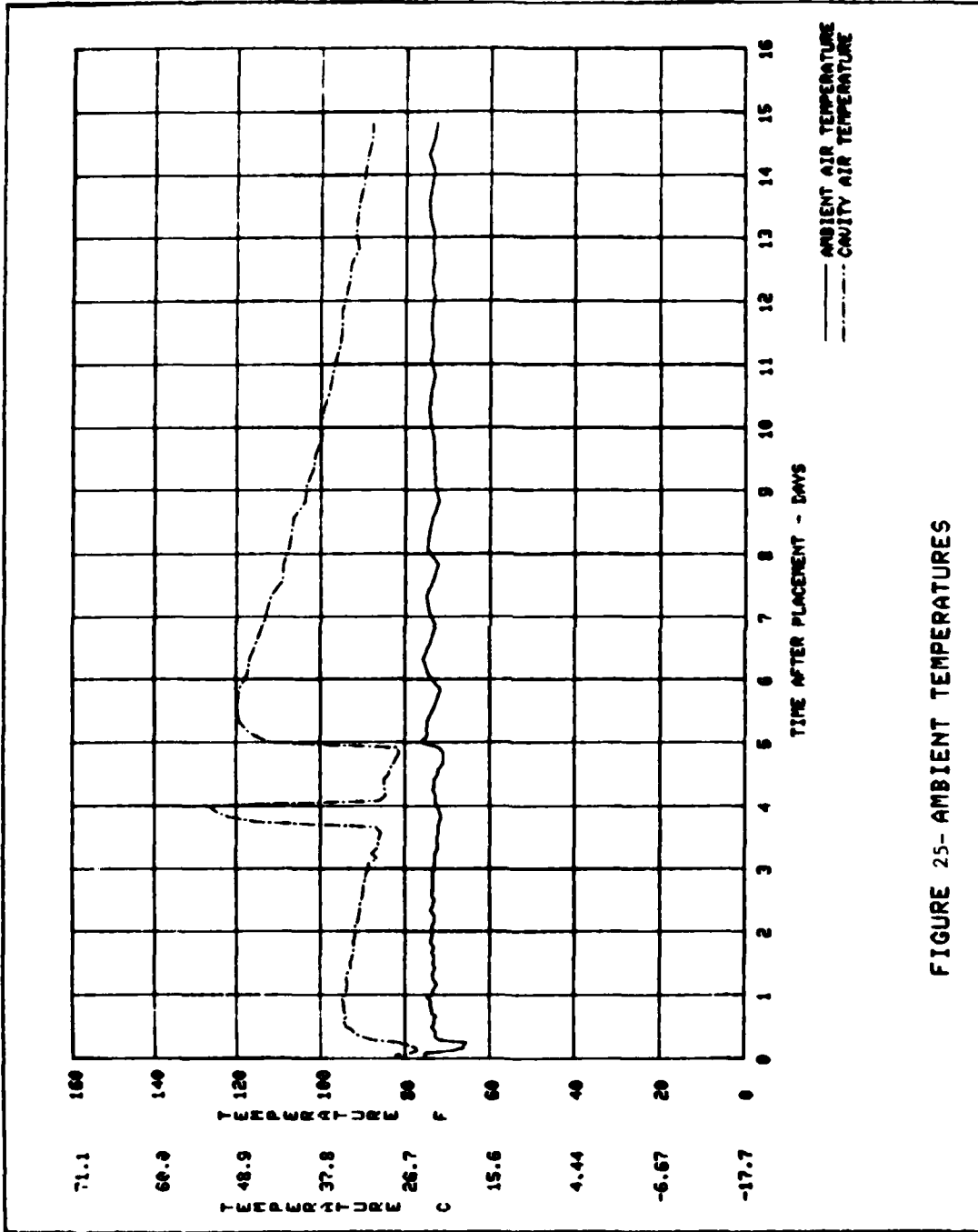


FIGURE 25- AMBIENT TEMPERATURES

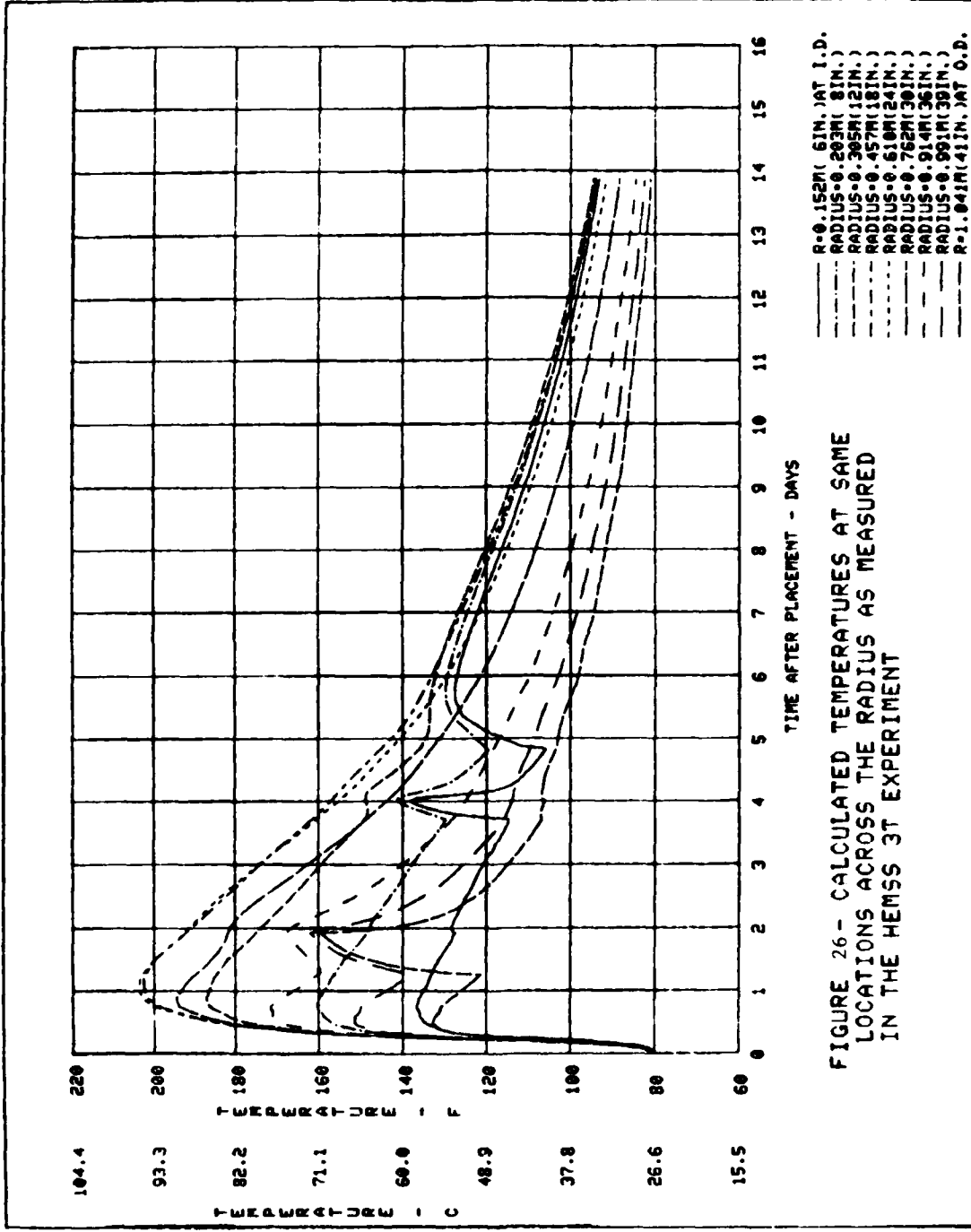


FIGURE 26- CALCULATED TEMPERATURES AT SAME
 LOCATIONS ACROSS THE RADIUS AS MEASURED
 IN THE HEMSS 3T EXPERIMENT

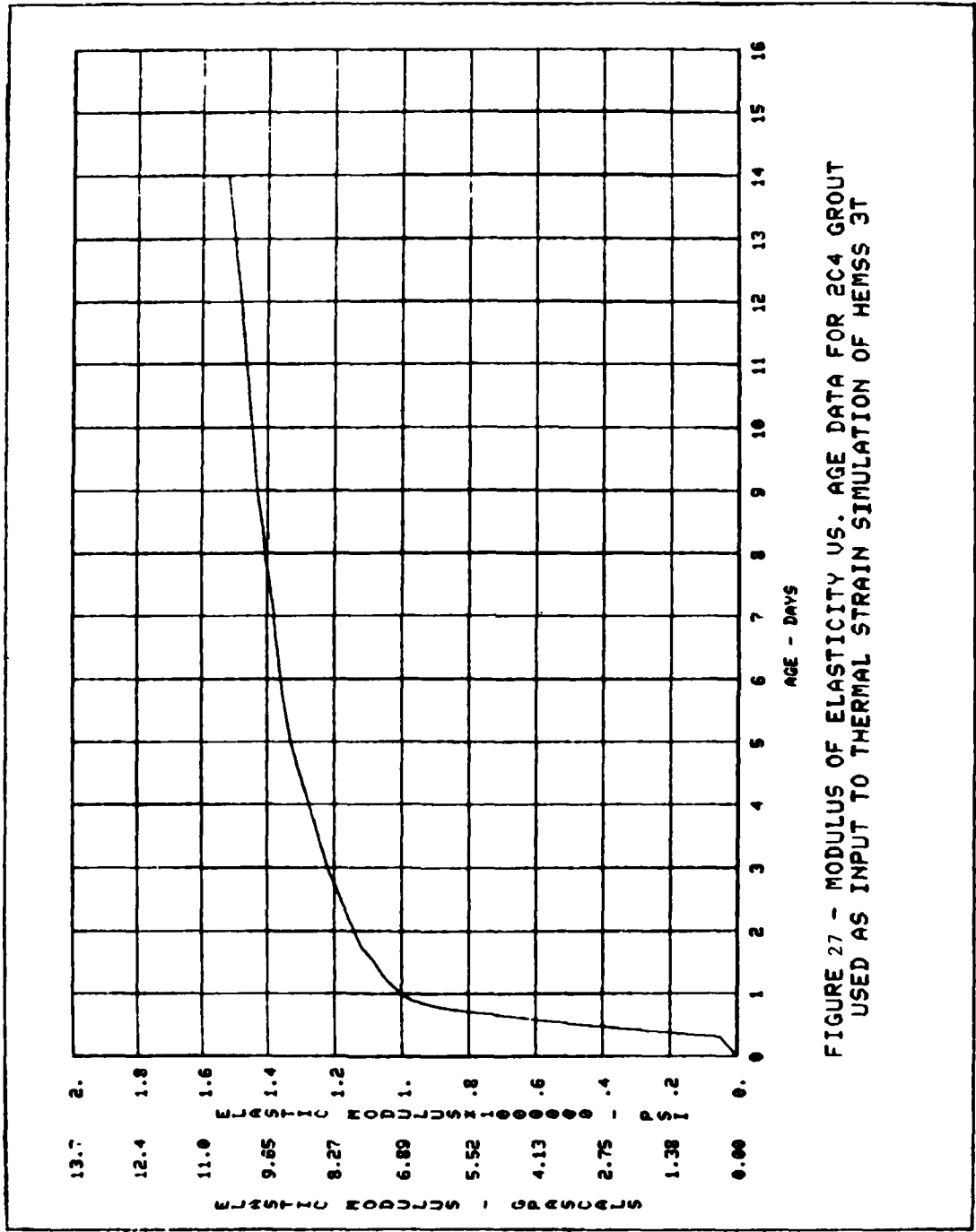
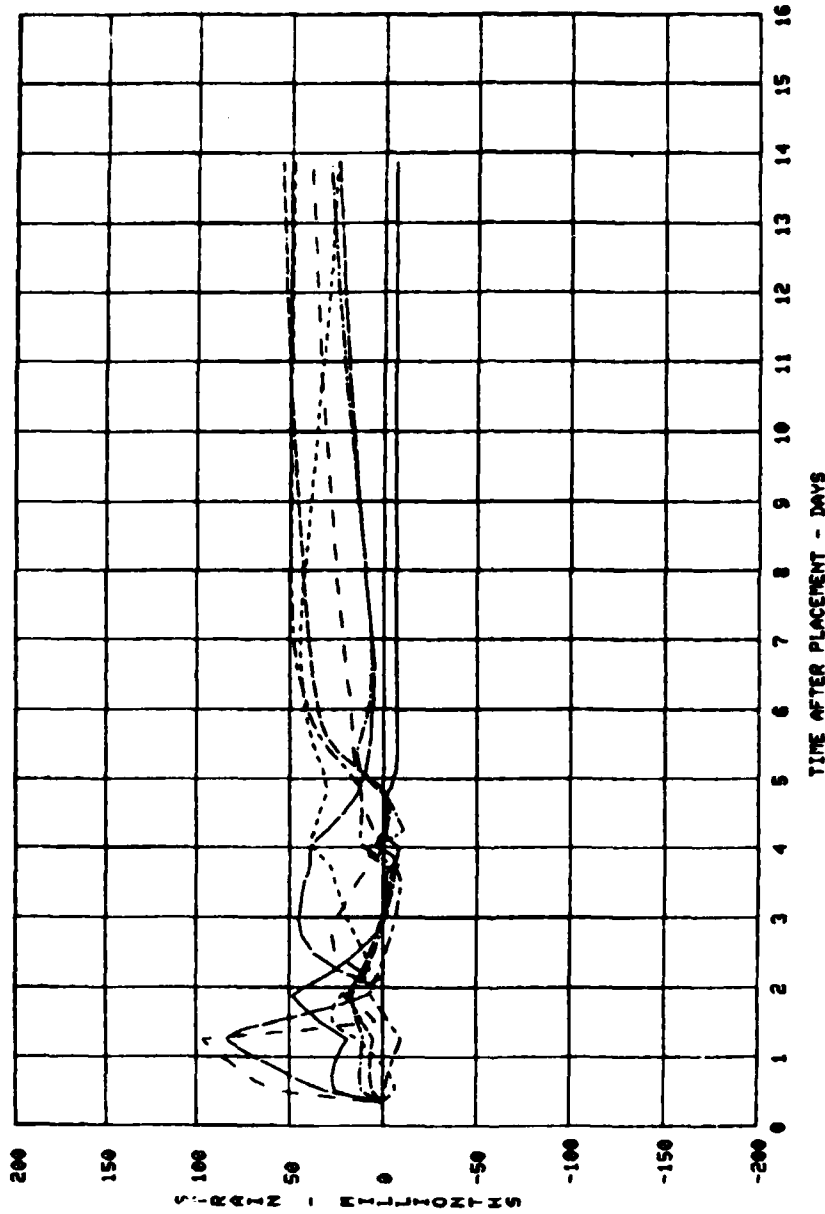


FIGURE 27 - MODULUS OF ELASTICITY VS. AGE DATA FOR 204 GROUT USED AS INPUT TO THERMAL STRAIN SIMULATION OF HEMSS 3T



- RADIUS=0.203IN.(8IN.)
- - - RADIUS=0.365IN.(12IN.)
- RADIUS=0.457IN.(18IN.)
- - - RADIUS=0.610IN.(24IN.)
- RADIUS=0.762IN.(30IN.)
- - - RADIUS=0.914IN.(36IN.)
- RADIUS=0.991IN.(39IN.)

FIGURE 28 - CALCULATED STRAINS(TANGENTIAL) AT SAME LOCATIONS AS MEASURED IN THE HEMSS 3T EXPERIMENT

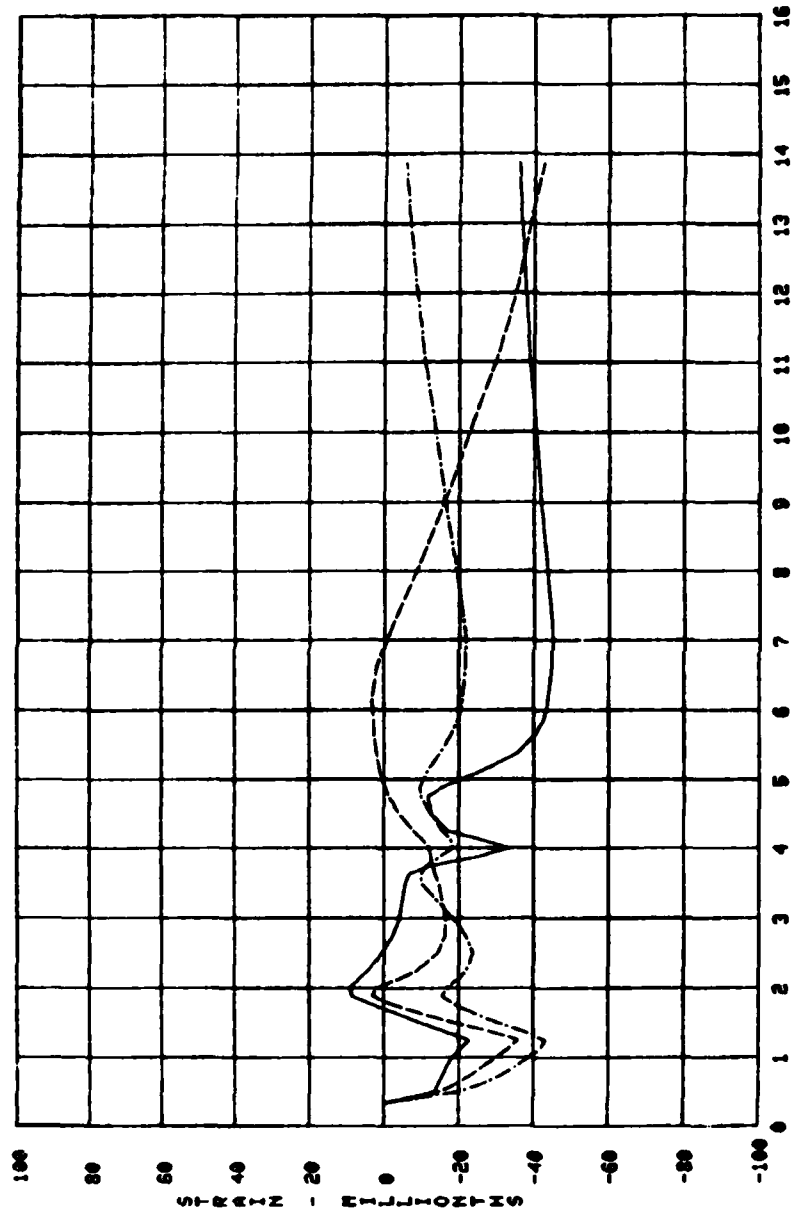


FIGURE 29 - CALCULATED STRAINS (RADIAL) AT SAME LOCATIONS AS MEASURED IN THE HEMSS 3T EXPERIMENT

In accordance with letter from DAEN-RDC, DAEN-ASI dated 22 July 1977, Subject: Facsimile Catalog Cards for Laboratory Technical Publications, a facsimile catalog card in Library of Congress MARC format is reproduced below.

Bombich, Anthony A.

The HEMSS 3T experiment / by Anthony A. Bombich (Structures Laboratory, U.S. Army Engineer Waterways Experiment Station). -- Vicksburg, Miss. : The Station ; Springfield, Va. ; available from NTIS, 1982.

67 p. in various pagings : ill. ; 27 cm. -- (CTIAC Report ; 57) (Miscellaneous paper ; SL-82-10)

Cover title.

"July 1982."

Final report.

"Prepared for Defense Nuclear Agency under DNA

Subtask Y99QAXSD070."

Bibliography: p. 17.

1. Grout (Mortar)--Testing. 2. Laboratory tests.
3. Concrete--Curing. 4. Temperature. I. United States.
Defense Nuclear Agency. II. U.S. Army Engineer Waterways
Experiment Station. Structures Laboratory. III. Title
IV. Series V. Series: Miscellaneous paper (U.S. Army

Bombich, Anthony A.

The HEMSS 3T experiment : ... 1982.
(Card 2)

Engineer Waterways Experiment Station) ; SL-82-10.
TA7.W34m no.SL-82-10